

“EQUIVALENT” MATERIAL PROPERTIES FOR DESIGNING IONIC POLYMER
METAL COMPOSITE ACTUATORS BY EQUIVALENT BIMORPH BEAM
THEORY

by
H. DİDEM ÇİLİNGİR

Submitted to the Graduate School of Engineering and Natural Sciences
in partial fulfillment of
the requirements for the degree of
Master of Science

Sabancı University
Spring 2008

“EQUIVALENT” MATERIAL PROPERTIES FOR DESIGNING IONIC POLYMER
METAL COMPOSITE ACTUATORS BY EQUIVALENT BIMORPH BEAM
THEORY

APPROVED BY

Assist. Prof. Dr. Melih Papila
(Thesis Advisor)

Prof. Dr. Yusuf Z. Mencelođlu

Assist. Prof. Dr. Mehmet Yıldız

Assist. Prof. Dr. Ayhan Bozkurt

Assist. Prof. Dr. Selmiye Alkan Gürsel

DATE OF APPROVAL:

© Halime Didem ÇİLİNGİR 2008

All Rights Reserved

“EQUIVALENT” MATERIAL PROPERTIES FOR DESIGNING IONIC POLYMER
METAL COMPOSITE ACTUATORS BY EQUIVALENT BIMORPH BEAM THEORY

Halime Didem ÇİLİNGİR

Materials Science and Engineering, MSc Thesis, 2008

Thesis Supervisor: Assist. Prof. Dr. Melih PAPİLA

Keywords: IPMC, Equivalent Bimorph Beam Model, Nastran, Finite Element Analysis

Abstract

This thesis addresses the Ionic Polymer Metal Composite (IPMC) actuators and two “equivalent” materials parameters for their design and performance assessments: electromechanical coupling coefficient and elastic modulus. The “equivalent” parameters not being material constants are derived from equivalent bimorph beam model. The Nafion membrane based IPMC actuator strips of several thicknesses are manufactured by electrochemical platinization method. The effect of the thickness and operating voltage on the equivalent coupling coefficient is demonstrated by using a design of experiment of three and five levels of the two factors, respectively. Experiments and finite element analyses using MD.NASTRAN are used to evaluate the tip displacement and the coupling coefficient for which response surface (RS) approximation as function of the thickness and voltage are constructed. Experiments and predictions indicate that thickness and voltage are interacting major factors for maximum tip displacement. The equivalent coupling coefficient is primarily driven by the thickness, and the voltage appears to contribute as the thickness increases. Initial curvature of the strips before excitation is also shown to be a factor for “equivalent” coupling coefficient, it is not, however sufficient to explain the variation in the experimental data. Correction factor approach is proposed and applied to the straight beam tip displacement RS that filters out experimental variation. Corrected RS enables to include the pre-imposed initial curvature as design parameter along with the actuator thickness and the operating peak voltage when predicting the tip displacement and the equivalent coupling coefficient. IPMC actuator “equivalent” elastic modulus is also determined by using blocking force data. The “equivalent” properties, electromechanical coefficient and young’s modulus

by the equivalent bimorph beam model works reasonably well in calculating the actuation force at the tip by MD.NASTRAN. These “equivalent” material properties can be easily implemented in preliminary design of actuator made of IPMC.

İYONİK POLİMER METAL KOMPOZİT EYLEYİCİLER İÇİN EŞDEĞER BİMORF
KİRİŞ KURAMI İLE "EŞDEĞER" MALZEME ÖZELLİKLERİ

Halime Didem ÇİLİNGİR

Malzeme Bilimi ve Mühendisliği, Y. Lisans Tezi, 2008

Tez Danışmanı: Doç. Dr. Melih PAPİLA

Anahtar kelimeler: İPMK, Eşdeğer Bimorf Kiriş Modeli, Nastran, Sonlu Elemanlar
Analizi

Özet

Bu tez çalışmasında, iyonik polimer metal kompozit (İPMK) eyleyiciler ile bu tip eyleyicilerin tasarım ve randıman değerlendirmeleri için iki “eşdeğer” malzeme parametresi: elektromekanik bağlaşım katsayısı ve elastik modülü ele alınmıştır. “Eşdeğer” parametreler malzeme sabiti olmayıp İPMK eyleyici tasarımında kullanılan eşdeğer bimorf kiriş modelinden türetilir. Nafion tabanlı iyonik polimer metal kompozit eyleyiciler farklı kalınlıklarda elektrokimyasal kaplama yöntemi ile üretildi. Membran kalınlığının ve çalıştırma voltajının katsayı üzerindeki kollektif etkisi deney tasarımı yöntemi kullanılarak söz konusu iki faktörün sırayla üç ve beş farklı düzeyleri kullanılarak incelendi. Uç deplasmanı ve elektromekanik bağlaşım katsayısını hesaplamak için deneysel çalışmalar ve MD.NASTRAN yazılımı ile sonlu elemanlar analizleri yapıldı. Böylece elektromekanik bağlaşım katsayı için kalınlık ve çalışma voltajının fonksiyonu olan vekil model çıkarıldı. Deneysel çalışmalar ve öngörüler eyleyici kalınlığı ve çalışma voltajının maksimum uç deplaman için temel faktörler olduğunu gösterdi. Eşdeğer elektromekanik bağlaşım katsayısının öncelikli olarak kalınlığa bağlı olduğu ve işlem voltajının da kalınlık artışı ile bağlantılı etki gösterdiği sonucuna varıldı. Ayrıca eşdeğer elektromekanik bağlaşım katsayısının eyleyicinin işlem voltajı uygulanmadan önceki şekline bağlı olduğu belirlendi. Bu bağ deneysel sonuçlardaki değişkenliğin açıklanmasında yeterli olmamakla birlikte düzeltme katsayısı yaklaşımı sunuldu ve düzlemsel kirişin uç deplasman vekil modeline uygulandı. Düzeltilmiş vekil model, başlangıç şeklini bir tasarım parametresi olarak eyleyici

kalınlıđının ve alıřma voltajının yanında ngrmeyi sađlar. Tm bu parametreler eyleyici u deplasmanı ve “eřdeđer” elektromekanik bađlařım katsayısının tahmininde kullanılabilir. Bunun yanında eyleyicinin bloke (hareket sınırlı) kuvvet verisinden yine “eřdeđer” bimorf kiriř modeli kullanılarak “eřdeđer” elaste modl hesaplanmıřtır. Konu edilen “eřdeđer” malzeme zellikleri, elektromekanik katsayı ve elastik modul eyleyici u kuvvet hesaplarında dođrulanmıřtır. Bu zellikler IPMC eyleyici n tasarımında kolaylıkla uygulanabilecektir.

Overview of thesis

Electroactive polymers (EAPs) are considered in the class of smart materials as they can exhibit controllable mechanical response when subjected to electric field. They find extensive application areas as actuators and sensors, including artificial muscle applications due to operational similarity to biological muscles. Electroactive Polymers are divided into two distinct groups based on their active mechanism, ionic and electronic EAPs and among the examples of ionic EAPs, ionic polymer metal composites (IPMCs) are in particular subject of this study. Beside their lightweight, low power consumption, compact design, fast response, noiseless motion and stability, they can also actuate under low operating voltages (1-5 V), display large bending deformation and operate both in air and wet conditions. The major formative material of IPMCs is ion exchange polymer membrane, typically Nafion[®] one with backbone ionomer perfluoro-sulfonate that is also widely used in hydrogen fuel cells. The IPMC actuator strips can be manufactured by following the process consisting of two main steps initial: compositing and surface electroding known as electrochemical platinization method. The method overall contains pretreatment of Nafion membrane, absorption (ion-exchange), primary plating (reduction), secondary plating, ion-exchange processes.

There are several models of various complexities to predict the response of IPMC actuators. One of the simple and easy to implement methods/models which may be suitable in design optimization is the “equivalent” bimorph beam model. The advantage of this approach is the fact that although the IPMC actuation is a transport phenomenon, it is treated as piezoelectric which is easier to model in commercial finite element analysis software such as MD.NASTRAN. An “equivalent” electro-mechanical coupling coefficient and “equivalent” young’s modulus can be expressed via the equivalent bimorph beam problem, and the IPMC is modeled for design purposes as if it is a piezoelectric material. It is important to label the coupling coefficient and young’s modulus “equivalent” or “effective” as they are dependent on several factors. In other words they are not an actual “material constants”. The coefficient, for instance varies with operating voltage and thickness that may be design parameters in number of problems.

The thesis work involved processing, characterization and modeling of the IPMCs to achieve the following objectives:

- To fabricate IPMC actuator strips from commercial Nafion[®] ion exchange membranes in various thicknesses.

- To investigate how the variables such as applied voltage, thickness, and initial curvature of the IPMC affect the “equivalent” electro-mechanical coupling coefficient and “equivalent” young’s modulus in equivalent bimorph beam approach.

The effects of different membrane thicknesses, applied voltage and frequency on the actuator characteristics are experimentally determined. Equivalent bimorph beam approach is utilized in such a way that experimental results and finite element analyses in MD. NASTRAN were integrated within the context of Response Surface Methodology (RSM) to obtain semi-empirical approximations for the equivalent material properties for preliminary design purposes.

The thesis starts with brief introduction on EAPs. A through review of IPMCs and their properties are provided in chapter 2. The highlight feature of IPMCs is their ability of actuation under low operating voltages (1-5 V) resulting large bending deformation. In chapter 3, materials that formed IPMC and manufacturing techniques are discussed. IPMC actuators, generally formed by the ion selective polymer membrane compositing with a noble metal such as platinum or gold as a thin layer on both surface and IPMC actuator strips can be manufactured by electroless plating or electrochemical platinization method.

Experimental and computational methods are explained in chapters 4 and 5, respectively. Application of a widely used fabrication method is defined in chapter 4. In computational part, “Equivalent” bimorph beam model is utilized for modelling IPMCs in commercial finite element analysis software named MD.NASTRAN. An “equivalent” electro-mechanical coupling coefficient and “equivalent” young’s modulus can be expressed via the equivalent bimorph beam problem, and the IPMC is modeled for design purposes as if it is a piezoelectric material. It is important to label the coupling coefficient and young’s modulus “equivalent” or “effective” as they are dependent on several factors. The results are then given and discussed in chapter 6 and finally chapter 7 offers the concluding remarks of the thesis work.

ACKNOWLEDGEMENTS

First of all I would like to thank my thesis supervisor Assist. Prof. Dr. Melih Papila for his guidance.

I would also like to thank the members of my advisory committee, Prof. Dr. Yusuf Mencelođlu, Assist. Prof. Dr. Mehmet Yıldız, Assist. Prof. Dr. Selmiye Alkan Gürsel, Assist. Prof. Dr. Ayhan Bozkurt, for reviewing my master thesis and gave me invaluable advices.

My sincere thanks to all my friends and colleagues, both in Mechatronics and Material Science programs, particularly A. Fatih TABAK who cooperated nicely during every step of my laboratory work, endless orientation advices both about university and masters program as a ‘science person’.

I would like to thank my family; S. Serpil ÇİLİNGİR for her desire to get over difficulties about life, Tufan ÇİLİNGİR for his unconditional support and Sinem ÇİLİNGİR for sharing wakeful nights with me, countless coffee breaks and social support with limitless song collection.

I am particularly grateful to U. Çađrı DOĐAN. Who would have known that you will also be my only inspiration through my life with starting with coincidences. Your constant and continuous co-operation always gives me enthusiasm to do better. The truth is without your help this study would never have been possible.

Finally, I kindly acknowledge the partial support for this work from the Sabanci University Internal Grant Program (contract number IACF06-00418).

TABLE OF CONTENTS

ABSTRACT	IV
ÖZET	VI
OVERVIEW OF THESIS	VIII
ACKNOWLEDGEMENTS	X
TABLE OF CONTENTS	XI
LIST OF FIGURES.....	XIII
LIST OF TABLES	XV
Chapter 1 INTRODUCTION	1
1.1. Electro-Active Polymers	3
1.1.1. Definition of EAPs	3
1.1.2. Structure and types of EAPs.....	4
1.1.3. Advantages&Disadvantages of ionic EAPs	6
Chapter 2 IONIC POLYMER METAL COMPOSITES	8
2.1. Brief History of IPMC Materials	8
2.2. Types of IPMC actuator materials	9
2.2.1. Aciplex	10
2.2.2. Flemion.....	10
2.2.3. Nafion®	11
2.2.3.1. Definition	11
2.2.3.2. Structure.....	12
2.2.3.3. Properties of Nafion®	15
2.2.3.4. Applications	17
2.3. Actuation mechanism in IPMC	17
2.3.1. Description of the mechanism.....	17
2.3.2. Enhancement of Actuation Performance.....	20
2.3.3. Factors affecting actuation	21
2.4. Types of predictive models for IPMC.....	22
2.4.1. Physical Models	22
2.4.2. Black-box Models	24
2.4.3. Gray Box Models	25
2.5. Pros and Cons for IPMCs.....	27
2.6. Applications of IPMCs.....	29

2.6.1.	Mechanical grippers	29
2.6.2.	Robotic swimming structure	31
2.6.3.	Composite wing flap	32
2.6.4.	Biomedical applications	32
Chapter 3	MATERIALS AND MANUFACTURING	34
3.1.	IPMC Materials	34
3.2.	Electroless plating	34
3.3.	Fabrication of solution recasted Nafion [®]	39
3.4.	Other potential techniques.....	39
Chapter 4	EXPERIMENTAL METHODS	42
4.1.	Unblocked Tip Displacement Experiments.....	42
4.2	Blocking Force Experiments	43
Chapter 5	COMPUTATIONAL METHODS	44
5.1	Equivalent bimorph beam model	44
5.2	Finite element analyses	46
Chapter 6	RESULTS AND DISCUSSION	50
6.1.	Surface Morphology.....	50
6.2	“Equivalent” electromechanical coupling coefficient by unblocked tip displacement study	53
6.2.1	Effect of IPMC thickness and applied voltage – quasistatic actuation	53
6.2.2	Finite element simulations of straight IPMC actuators.....	56
6.2.3	Finite element simulations of curved IPMC actuators - Effect of initial curvature 58	
6.2.4	Effect of frequency	63
6.3.	“Equivalent” Young’s Modulus by unblocking force study	64
6.3.1	Finite element simulations of straight IPMC actuators for force measurement.	65
Chapter 7	CONCLUSION	67
7.1	Concluding remarks	67
REFERENCES	68

LIST OF FIGURES

Figure 1.1 An illustration of the Piezoelectric Effect [3]	3
Figure 2.1 Perfluorinated ionomers used in IPMC manufacture include (a) Aciplex, (b) Flemion, and (c) Nafion [®]	9
Figure 2.2 Chemical structure of Nafion [®] polymer	13
Figure 2.3 Schematic representation of cluster network model	14
Figure 2.4 Ionic distribution of cluster network model.....	15
Figure 2.5 A schematic diagrams of the typical IPMC actuator and its actuation principle....	19
Figure 2.6 Actuation of typical IPMC under an applied voltage varied with time	21
Figure 2.7 Bending principle and angle of IPMC	25
Figure 2.8 Equivalent circuit for the gray box model presented by Kanno et al [79].....	25
Figure 2.9 Typical IPMC actuator.....	27
Figure 2.10 Example of multi finger gripper	30
Figure 2.11 Demonstration of IPMC wipers used by NASA/JPL.	31
Figure 2.12 A designed and fabricated undulating caudal fin actuator and two robotic fish equipped with IPMC fin actuator	31
Figure 2.13 Schematic representation of composite wing flap	32
Figure 2.14 from biological muscles to artificial ones.....	33
Figure 3.1 A schematic representation of IPMC after first and second plating processes.....	37
Figure 3.2 Scheme for IPMC fabrication: (1) ion exchange with noble metal salt; (2) reduction of metal at surface; (3) ion exchange with desired cation.....	38
Figure 4.1 Interface of the image processing software	42
Figure 4.2 Experimental setup of Blocking Force.	43
Figure 5.1 Equivalent bimorph beam model.....	44
Figure 5.2 Finite element model of IPMC	46
Figure 5.3 Defining the materials of layers.....	47
Figure 5.4 Defining composite material.....	48
Figure 5.5 Applying initial temperature to IPMC	49
Figure 5.6 Applying temperature to IPMC	49
Figure 6.1 AFM results of IPMC actuator surface.....	50
Figure 6.2 SEM analyze of IPMC	51
Figure 6.3 Example of surface crack which is detect by SEM	51
Figure 6.4 EDS measurements through whole structure of IPMC actuator.....	52
Figure 6.5 EDS measurements of IPMC actuator	53

Figure 6.6 Unblocked Tip displacement – voltage relationship for various thicknesses.....	54
Figure 6.7 Finite element analyses and experimental results for thickness of 70 μ m thick IPMC test specimen at applied voltage 1 V 70 μ m at 1 and 2 Volts, resulting in 1.667 mm and 3.334 mm, respectively (Test 2 column of Table 6.1).	57
Figure 6.8 Prediction contours, Tip displacement, s_{av} (Left) and Equivalent coupling coefficient, d_{31} (right).	57
Figure 6.9 The curved IPMC strip used in the experiments.....	58
Figure 6.10 Finite element models of beams.....	59
Figure 6.11 Finite element results for curved (left) and straight beam (right).....	60
Figure 6.12 Variation of the correction factor versus initial radius of curvature.....	62
Figure 6.13 Frequency vs. tip displacement graphs	63
Figure 6.14 Finite Element result.....	65
Figure 6.15 Modelling of rigid surface and contact.....	66
Figure 6.16 Force acting to the rigid surface	66

LIST OF TABLES

Table 1.1 List of the leading EAP materials[9].....	5
Table 1.2 Summary of the advantages and disadvantages of the two basic EAP groups [9]	7
Table 6.1 Measured free tip displacements according to various thicknesses and voltage values.....	54
Table 6.2 Comparison of electro-mechanical coupling coefficients obtained by Eq. 5.4 (with s_{av}) and Eq. 6.2 (with \hat{s}_{av})	56
Table 6.3 Initial curvature effect and correction on equivalent coefficient, the tip displacement of the straight beam analysis $s_{\text{straight}} = 4$ mm, and associated coefficient $d_{31} = 4.267 \times 10^{-2} \mu\text{m/V}$ due to Eq.(5.4) when 1V is applied.....	61
Table 6.4 Geometric and Characteristic values of IPMC actuator.....	64

CHAPTER 1 INTRODUCTION

Until recent times, most of the known engineering materials and structures (e.g. steel, aluminum) give only limited responses to external conditions. Why responses are defined as limited is that structures and materials are optimized to accomplish range of scenarios to which a structure may be exposed, this yield a structure which does not give the best response for any set of conditions. For instance, when the wings of an aircraft are designed, all scenarios are taken into consideration so to optimize the performance of wings. This optimization according to the all scenarios leads to loosing in best response to a specific scenario such as landing. That is why passenger aircrafts create additional lift surface during landing.

The engineering materials which are considered as most flexible materials are advanced composites. Since choosing the orientations, composition and density of fibers make it possible to create a composite material meet the requirements of design criteria. However, for these materials the final engineering structure is only for one application.

On the other hand, in the natural world this is antipodean. In order to survive, animals and plants can adapt to their surroundings. Their perfect abilities have always been inspiration for the scientists and engineers. This field of engineering is called as biomimetics which is extraction of engineering design concepts from natural world. And it is obvious that there are too much things to gain from this field for future manmade materials.

In order not to use smart structures and smart materials terms erroneously, it is firstly better to look into the meaning of these terms in detail.

Structures can be considered as smart if they are capable of giving responses to the changes in their environment. For example, it may be self repairing or it may use variable stiffness elements to control its response to applied mechanical loads.

A lot of examples from natural world can be compiled which can be thought as smart structures. Some of them can be listed as allowing leaf surfaces to follow the direction of sunlight, limping to avoid overload of a damaged region by changing in the load path through the structure and reflex to heat and pain. From an engineering point of view, this process of balance is a smart response, allowing a flexible structure to adapt its form to minimize the effects of an external force, thus avoiding tragic results.

Actually, the materials and structures involved in natural world are really smart since they first sense the changes in their environment, then they are processing this data and give

responses according to the processed data. This is an amazing process since they integrate engineering judgment and information technology in order to give quick and appropriate responses.

As it is mentioned above, list of the examples for smart structures can be extended. By the same logic, some materials have the capability to change one or more properties such as shape according to the changes in the external conditions such as voltage, temperature, pH or magnetic fields. These kinds of materials are thought as smart materials. Since these materials give responses to the external conditions, they are often called as responsive materials. All materials are actually responsive. But being a smart material is something different. Responsivity is having the same output information for as the input which is the principle of transducer technology. However to consider a material as smart, this material should give specific response to a combination of inputs. This is the criteria of smartness [1].

According activation mechanism, smart materials can be classified into four main groups;

Electroactive materials such as piezoelectric materials are smart materials since they produce voltage with the applied stress. Also reverse of this is possible for these materials. A voltage across the sample will produce stress within the sample. This feature can be utilized to obtain structures bending, expanding or contracting when a voltage is applied (Figure 1.1).

Shape memory alloys and shape memory polymers are considered as thermo-responsive materials where deformation can be induced and recovered through temperature changes.

Magnetic shape memory alloys are smart materials since they change their shape with the change in the magnetic field.

pH-sensitive polymers are materials which swell/collapse according to change of the pH of the surrounding media.

Chromogenic systems have ability to change colour in response to electrical, optical or thermal changes. The types of chromogenic systems are;

- Electrochromic materials, when voltage is applied this kind of materials they change their colour or opacity. Liquid crystal displays are example of electrochromic materials
- Thermochromic materials change their color depending on temperature
- Photochromic materials gave response to light which for instance, light sensitive sunglasses that darken when exposed to bright sunlight.

- Non-Newtonian fluid is a substance that changes its viscosity in response to an applied shear rate. In other words the liquid will change its viscosity in response to some sort of force or pressure is other well known types of smart materials [2].

The focus of this thesis is on a type of Electroactive materials: Electroactive polymers. They are most widely used as sensors in different environments. For instance to measure fluid compositions, fluid density, fluid viscosity, or the force of an impact. An example of an electroactive sensor in everyday life is the airbag sensor in cars. The material senses the force of an impact on the car and sends an electric charge deploying the airbag [3].

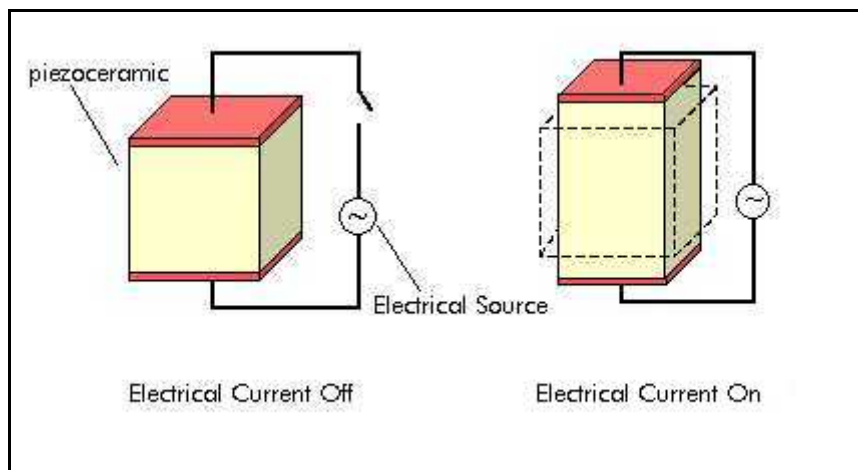


Figure 1.1 An illustration of the Piezoelectric Effect [3]

1.1. Electro-Active Polymers

1.1.1. Definition of EAPs

One of the widely considered types of smart materials is electroactive polymers (EAPs), polymeric materials, simply whose shapes are modified when a voltage is applied on them. The reason why large numbers of research and development efforts have been dedicated to the field of electro active polymers (EAPs) in the last several years is their impressive advantages; high strain capability (large amount of deformation while sustaining large forces), similarities with biological tissues in terms of achievable stress and force, inherent flexible and durable nature, easy processing, long life and low cost are the most attractive ones among them. These extraordinary advantages make them good candidates to potential applications of electromechanical devices, robotics, planetary, liquid and gases flow control, control weaving, micro electro mechanical systems (MEMS), human machine interfaces, sensors and actuators.

The markets for EAP devices are strongly driven by the expanding medical market, E-textiles and robotics with its demand for a novel class of electrically controlled actuators based on polymer materials.

In addition to these, EAP actuator has potential applications in areas where flexibility of a moving system and accurate control of the motion should goes together such as: highly developed consumer products like smart fabrics, toys and medical technology [4].

1.1.2. Structure and types of EAPs

Electroactive polymers (EAPs) divided into two distinct groups based on their active mechanism as can be seen from Table 1.1. First one, electronic EAPs display response according to their electronic active group. Coulomb forces drive the electronic EAP, which include electrostrictive, electrostatic, piezoelectric and ferroelectric. This type of EAP materials can be made to hold the induced displacement while activated under a DC voltage, allowing them to be considered for robotic applications. These EAP materials have a greater mechanical energy density and they can be operated in air with no major constraints. However, the electronic EAP require a high activation fields ($>100\text{-V}/\mu\text{m}$) that may be close to the breakdown level [5-6].

Table 1.1 List of the leading EAP materials [9]

Electronic EAP	Ionic EAP
Dielectric EAP	Carbon Nanotubes (CNT)
Electrostrictive Graft Elastomers	Conductive Polymers (CP)
Electrostrictive Paper	ElectroRheological Fluids (ERF)
Piezoelectric EAP	Ionic Polymer Gels (IPG)
Ferroelectric Polymers	Ionic Polymer Metallic Composite (IPMC)
Liquid Crystal Elastomers (LCE)	

Second one also implies the group of materials related with the content of this thesis work, ionic EAP. General characteristic is explained as they have electrolyte which ions /molecules depart in response to applied electric field. In other words actuation is caused by the displacement of ions inside the polymer.

Each of the groups and individual type of EAP materials has its advantages and disadvantages that need to be taken into account when considering applications. The induced

displacement of both the electronic and ionic EAP can be designed geometrically to bend, stretch or contract. Any of the existing EAP materials can be made to bend with a significant bending response, offering an actuator with an easy to see reaction. However, bending actuators have relatively limited applications due to the low force or torque that can be induced. EAP materials are still custom made mostly by researchers and they are not available commercially [7].

In ionic EAPs, transportation of ions inside the polymer causes actuation. The term ion exchange polymers refers to polymers designed to selectively exchange ions of a single charge either cations or anions with their own incipient ions. Fixed covalent ionic groups are the base structure of that type of polymers. They are often manufactured from typical ion exchange polymers which are described in the following.

- (i) Perfluorinated alkenes with short side-chains terminated by ionic groups (typically sulfonate or carboxylate (SO^{-3} or COO^{-}) for cation exchange or ammonium cations for anion exchange. In the structure determination of mechanical strength is provided by large polymer backbones. On the other hand short side-chains supply ionic groups that interact with water and the passage of appropriate ions.
- (ii) Styrene/divinylbenzene-based polymers in which the ionic groups have been substituted from the phenyl rings where the nitrogen atom is fixed to an ionic group. The characteristic properties of these polymers are that they are highly crosslinked and rigid. Actuation is able to provide by only a few volts are needed for, but the ionic flow implies a higher electrical power needed for actuation. On the other hand energy is needed to keep the actuator at a given position.

Examples of ionic EAPs are conducting polymers, bucky gel actuator, responsive gels, ionic polymers in a composite form with a conductive medium such as a metal herein called ionic polymer metal composites (IPMCs), can exhibit large dynamic deformation if suitably electroded and placed intages of a time-varying electric field. Conversely, dynamic deformation of such ionic polymers produces dynamic electric fields across their electrodes [8].

1.1.3. Advantages&Disadvantages of Ionic EAPs

Being able to produce large bending displacements with low voltage is the key advantage of these materials. Also they display bi-directional actuation that depends on the voltage polarity, naturally.

Table 1.2 Summary of the advantages and disadvantages of the two basic EAP groups [9]

EAP type	Advantages	Disadvantages
Electronic EAP	<ul style="list-style-type: none"> • Exhibit rapid response (milliseconds) • Can hold strain under dc activation • Induces relatively large actuation forces • Exhibits high mechanical energy density • Can operate for a long time in room conditions 	<ul style="list-style-type: none"> • Requires high voltages (~100 MV/meter). • Independent of the voltage polarity, it produces mostly monopolar actuation due to associated electrostriction effect.
Ionic EAP	<ul style="list-style-type: none"> • Natural bi-directional actuation that depends on the voltage polarity. • Requires low voltage • Some ionic EAP like conducting polymers have a unique capability of bi-stability 	<ul style="list-style-type: none"> • Requires using an electrolyte • Require encapsulation or protective layer in order to operate in open air conditions • Low electromechanical coupling efficiency • Except for CPs and NTs, ionic EAPs do not hold strain under dc voltage • Slow response (fraction of a second) • Bending EAPs induce a relatively low actuation force • Electrolysis occurs in aqueous systems at >1.23 V

By the way disadvantages of ionic EAPs are not hold strain under DC voltage, show relatively slow response (fraction of a second) and low actuation force. Also it is difficult to produce a consistent material particularly for IPMCs. On the other hand in aqueous system the materials sustain electrolysis over 1.23V and also need for an electrolyte and encapsulation beside all of these they have low electromechanical coupling efficiency [7, 9, 10, 11].

As indicated above among ionic EAPs, IPMCs are main research field of this work. The major formative material of IPMCs is ion exchange polymer membrane, widely used in

hydrogen fuel cells in order to produce sodium or potassium hydroxide in other words ion separation.

CHAPTER 2 IONIC POLYMER METAL COMPOSITES

2.1. Brief History of IPMC Materials

In 1939s polymer metal composites were first developed by the use of the precipitation of colloidal silver on prepared substrates [12]. One thing to add that, these early materials suffered from delamination of the metal overlayer. After that, sputtering methods have provided routes to polymer metal composites, but these were cause to delamination as well [13,14].

A field of shape-modifying polymers dates back more than 50 years. EAP is one of these polymers and also IPMC s are a kind of them. To highlight the elements that distinguish IPMC materials from other electroactive polymers. One of the most significant aspects of IPMCs is their actuation based on the active motion of ions and solvent molecules within the membrane under applied stimulus. This motion is directionally dependent and always occurs only in one direction and other materials whose actuation derives from the passive (isotropic, volumetric) response to stimuli.

Without a doubt, the permselective properties of ionomeric resins could be used to make possible selective reduction of metal salts at the surface of an ion exchange membrane using chemical reductants such as sodium borohydride (NaBH_4) or hydrazine (N_2H_4) [15] was discovered near the end of 1960s by researchers at Dow Chemical. Later, both that permselective properties and preparation methods were applied to Nafion-type membranes by many Japanese groups, as well as workers at Hitachi [16, 17, 18] in the early 1980s. Millet and coworkers further developed the technique of IPMC formation, characterizing the plating mechanism to improve the morphology of the metal electrodes in IPMCs [19-23].

IPMC actuators were first developed as solid polymer electrolyte membranes for fuel cells [24]. The aim of those investigations is to use them as hydrogen pressure transducers, researchers Sadeghipour et al. [25] for fuel cell applications. They found that IPMC materials could act as vibration sensors. They also reported that a traditional platinum coated IPMC in the Na^+ ion form able to generate over 12 mV/g of acceleration in optimum experiment conditions. In addition to these, they investigate the dynamic behavior of their “cell” filters and amplify vibratory input to the IPMC, and that the signal response of the IPMC is not strongly frequency dependent. In noting that the transduction of ions in selective polymer membrane generates a voltage and credited for proposing this material as a soft sensor by

Sadeghipour and coworkers. It should be noted that this investigation was closest to discovering IPMCs use as an actuator [25].

At the same time, in Japan, Oguro et al. described the ability of an IPMC material to bend under an applied electric field [26]. Not only in Japan but also in the USA, researchers, such as Mojarrad and Shahinpoor [27], have since sought to improve the performance of Nafion[®]-based IPMC actuators through optimization of the method of fabrication, including electrode morphology, dimensions sample size. More recently, Nemat- Nasser [28], Nemat-Nasser and Wu [29], and Nemat-Nasser and Zamani [30] have performed through and systematic studies of the properties and actuation of both Nafion[®]- and Flemion-based IPMCs, in various cation forms and with different solvents, seeking to identify at the bottom of the mechanisms of actuations, in order to model the phenomena of the IPMC actuation and quantitatively sensing properties and relate these to the composition, processing and microstructure of IPMC materials[31].

2.2. Types of IPMC actuator materials

After that brief history about IPMC actuators traditional definitions related to that field, fabrication processes and upcoming optimization ways have become definite. In order to give a definition of IPMC actuators, generally the ion selective polymer membrane compositing with a noble metal such as platinum or gold as a thin layer on both surfaces, produce IPMCs. Although there are several ionic polymer membranes used in IPMCs, Nafion[®] (E. I. Du Pont de Nemours and Company, Inc.) is the most widely known and used one with backbone ionomer perfluoro-sulfonate. On the other hand the backbone of polymer can be perfluoro-carboxylate group so other common polymer membrane Flemion[®] (Asahi Glass) formed not only these but also one rarely used polymer membrane known in literature called Aciplex[®] (Asahi Chemical) [31].

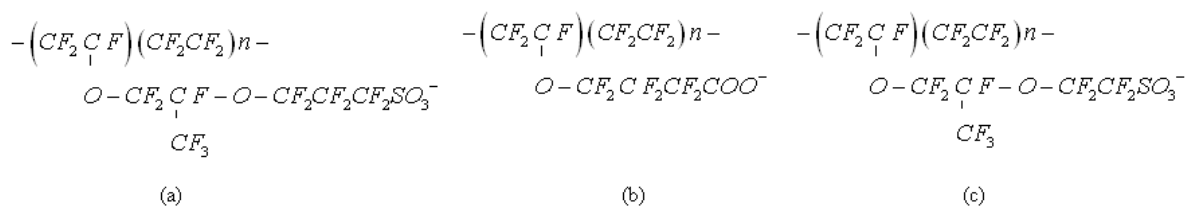


Figure 2.1 Perfluorinated ionomers used in IPMC manufacture include (a) Aciplex[®], (b) Flemion[®], and (c) Nafion[®]

Figure 2.1 displays the chemical structure of three perfluorinated ionomers used to produce IPMCs that mentioned paragraph above, that can easily seen, three of them varying in the length, side chain number and in the nature of ionic side group (usually sulfonate or carboxylate anions). On the other hand the acidity strength of the ionic side group has a profound effect on the actuation of the resulting IPMCs and, indeed, lies at the root of the back-relaxation mechanism in Nafion[®]-based IPMCs.

2.2.1. Aciplex

Asahi Kasei Company began the first commercial chlor-alkali production using the membrane electrolysis process in 1975. After that date they have continued to lead the world in pioneering the development of membrane electrolysis technology, especially the Aciplex[®] perfluorosulfonic acid membrane. The advantage of that membrane production process with using chlor-alkali electrolysis eliminates the need for mercury and asbestos as process materials, and enables greater energy efficiency. That superiority of Asahi Kasei chlor-alkali process technology has been recognized throughout the world, and the Aciplex[®] membrane is employed in plants with a total production capacity of over 5 million tons of caustic soda (sodium hydroxide) per year [32].

2.2.2. Flemion

The Asahi Glass Group (AGC) has been fully meeting the needs of the times concerning environmental friendliness and safety regarding its caustic soda (sodium hydroxide) production process. Caustic soda is an indispensable chemical for a variety of industries and is used in the production of diverse products, including chemical fibers, paper and pulp, and soaps. Caustic soda is manufactured by the electrolysis of brine, and the mercury process and the asbestos diaphragm process were traditionally used in its manufacture. However, due to the pollutive effects of mercury and asbestos emissions into the environment, early in the 1970s, the Japanese government required domestic manufacturers to develop a new manufacturing process for caustic soda.

In 1974, in response to the government request, the AGC Group embarked on the development of an ion-exchange membrane process, in which the electrolysis of brine is conducted using an ion-exchange membrane for selective filtering of ions to produce caustic soda and chlorine. Subsequently in 1975, Asahi Glass developed a fluoropolymer ion-exchange membrane (Flemion[®]) to be used for caustic soda production. They also developed highly durable and energy-saving activated cathodes, and established the electrolysis

technology to manufacture caustic soda by the use of Flemion[®] and the activated cathodes. The ion-exchange membrane process does not require the use of hazardous substances. Also, the process leads to substantial energy saving. The AGC Group, by the use of this newly developed manufacturing process with these advantageous features, has achieved an approximately 40% reduction in energy consumption as compared to the mercury process and the diaphragm process.

Although, Flemion has higher ion exchange capacity, higher stiffness, and greater water uptake than Nafion[®] Flemion based IPMCs actuation mechanism differs with no back relaxation. That is because of alkali metal cations in Flemion[®] shows fast initial bending towards the anode, followed by a slow motion in the same direction, but in the Nafion[®] based IPMC initial fast bending towards the anode followed by slow relaxation in the opposite direction. When wetted and small time varying alternating current (AC) applied on IPMC, it shows a large bending vibration at the applied frequency.

The electrical-chemical-mechanical response of the IPMCs depends on the neutralizing cation, the nature of the solvent and the degree of saturation, the electrode morphology, and the chemical structure and characteristics of the polymer backbone [33].

2.2.3. Nafion[®]

2.2.3.1. Definition

Basically, Nafion[®] is the sulfonated tetrafluorethylene copolymer, which is developed by Walther Grot of DuPont de Nemours, in the early 1970s.

Nafion[®] is composed of carbon-fluorine backbone chains and perfluoro side chains containing sulfonic acid groups with a molecular formula $C_7HF_{13}O_5S \cdot C_2F_4$. Nafion[®] has a unique numerical identify number (CAS No.) [31175–20–9][34].

The molecular weight of Nafion[®] is not certain due to differences in processing and solution morphology. The molecular weight variability of the material can be seen from Figure 2.2 which is the structure of a Nafion[®] unit; for example, the most basic monomer contains chain variation between the ether groups [35-36].

Determining molecular weight with conventional methods such as light scattering and gel permeation chromatography are not applicable to Nafion[®], since Nafion[®] is insoluble, although the molecular weight has been estimated as 10^5 - 10^6 Da. [37-38]. Because of that, the equivalent weight (EW) and material thickness are used to describe most commercially

available membranes. The EW is defined as the weight of Nafion[®] per mole of sulfonic acid group. For example, Nafion[®] 117 represents 1100 g EW + 0.007 inch in thickness.

In addition to equivalent weight, conventional ion-exchange membranes are usually described in terms of their ion exchange capacity (IEC) which is inversely proportional to the equivalent weight [39].

2.2.3.2. Structure

Common definition of IPMC is selective ion exchange membrane that plated on both sides with a noble metal such as gold or platinum and neutralized with the necessary amount of counterions that balance the electrical charge of anions which are covalently fixed to the backbone ionomer [40]. After that definition structure of selective ion exchange membrane should be examined in detail.

Nafion[®] is the first of a class of synthetic polymers with ionic properties which are called ionomers. In other words; Nafion[®] is perfluoro-sulfonated ionomers membrane. Incorporation of perfluorovinyl ether groups terminated with sulfonate groups onto a tetrafluoroethylene (Teflon) backbone make Nafion[®] unique in ionic properties. Typically, these membranes are manufactured from polytetrafluoroethylene as an effective backbone and sidechains ending with active ion-exchange sites with sulfonate. In other words, the microstructure of Nafion[®] consists of three regions:

- (i) a polytetrafluoroethylene (PTFE, DuPont's Teflon[™])-like backbone or the hydrophobic fluorocarbon backbone,
- (ii) side chains of $\text{---O---CF}_2\text{---CF---O---CF}_2\text{---CF}_2\text{---}$ which connect the molecular backbone to the third region, that is to say interfacial region,
- (iii) ion clusters consisting of sulfonic acid ions or hydrophilic anionic clusters of sulfonic acid groups. The third region is consist of few fixed ionic groups, which are located at the end of side chains so as to position themselves in their preferred orientation to some extent. Therefore they can create hydrophilic nanochannels, so called “cluster networks” or simply “ionic clusters”. Such configurations are completely different in other ionic polymers such as styrene/divinylbenzene families that are primarily limited by crosslinking, the ability of the ionic polymers to expand (due to their hydrophilic nature).

The starting monomer is the perfluorinated alkenes with appropriate substituents. An important consideration is the length of the sidechain that determines the properties of the final product. In general, the overall process is nontrivial in the fact that sulfonylfluoride vinyl ether is copolymerized with tetrafluoroethylene and then base-hydrolyzed to become an active material [41].

Protons on the sulfonic acid (SO_3H) groups "hop" from one acid side to another. Because of the membrane nature, pores allow movement of cations but the membranes do not conduct anions or electrons.

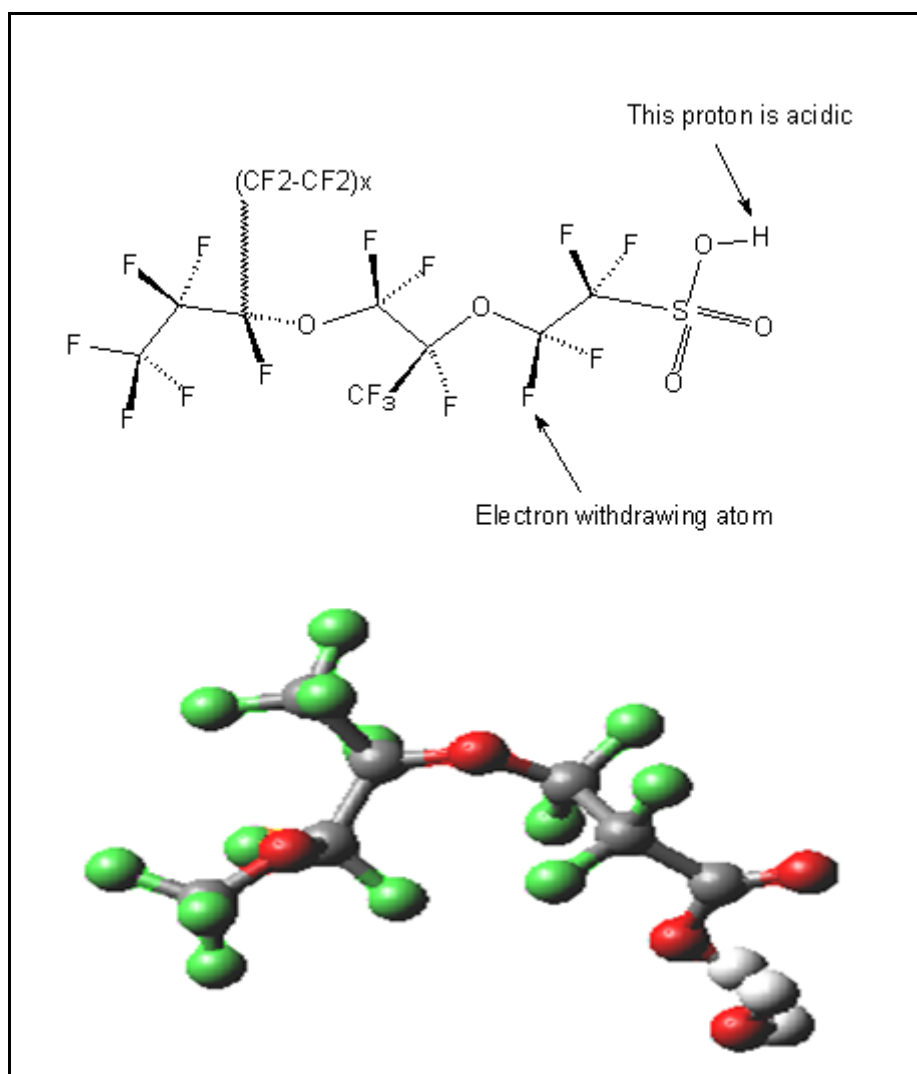


Figure 2.2 Chemical structure of Nafion[®] polymer

The morphology of Nafion[®] membranes is a matter of continuing study to allow for greater control on its properties. Other properties must be related to the Nafion[®] structure such as water management, hydration stability at high temperatures, electro-osmotic drag, as well as the mechanical, thermal, and oxidative stability.

Nafion[®] belongs to the wide class of solid superacids catalysts, in that it exhibits acid strength greater than that of 100% H₂SO₄. It has hydrophobic (-CF₂-CF₂-) and hydrophilic (-SO₃H) regions in its polymeric structure, and its superacidity is attributed to the electron-withdrawing effect of the perfluorocarbon chain acting on the sulfonic acid group. Nafion[®] is able to catalyze various reactions, such as alkylation, disproportionation and esterification [42, 43].

The model for Nafion[®] morphology, called the Cluster-Channel or Cluster-Network Model, consisted of an equal distribution of sulfonate ion clusters (also described as 'inverted micelles') with a 40 Å (4 nm) in diameter held within a continuous fluorocarbon lattice. In addition to that clusters are actually in contact with each other. In Nafion[®]-based IPMCs in alkali cation forms these narrow channels about 10 Å (1 nm) in diameter interconnect the clusters, which explain the transport properties [38, 39, 44].

Also cations rather than their solvation, water molecules are of primary importance in the IPMC actuation.

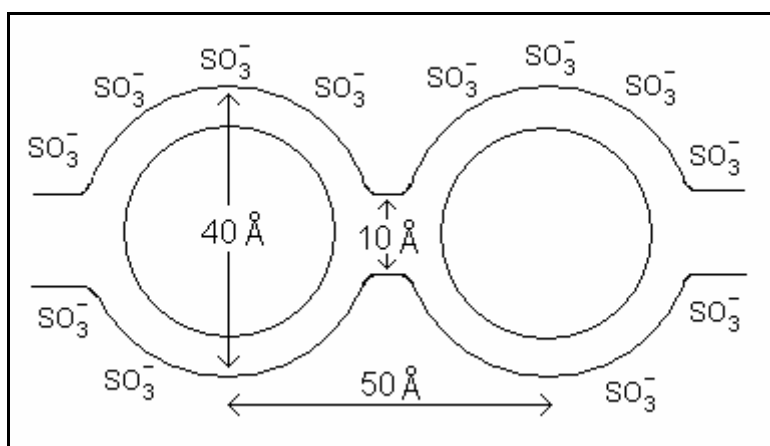


Figure 2.3 Schematic representation of cluster network model

Determining the exact structure of Nafion[®] is difficult because of Nafion[®] stems has inconsistent solubility and crystalline structure among its various derivatives. Advanced morphological models have included a core-shell model where the ion-rich core is surrounded by an ion poor shell, a rod model where the sulfonic groups arrange into crystal-like rods, and a sandwich model where the polymer forms two layers whose sulfonic groups attract across an aqueous layer where transport occurs.

Similarity between the models is a network of ionic clusters; on the other hand they differ in the cluster geometry and distribution from each other. Although no model was yet

determined fully correct, some scientists have demonstrated that as the membrane hydrates, Nafion[®]'s morphology transforms from the Cluster-Channel model to rod-like model. [37]

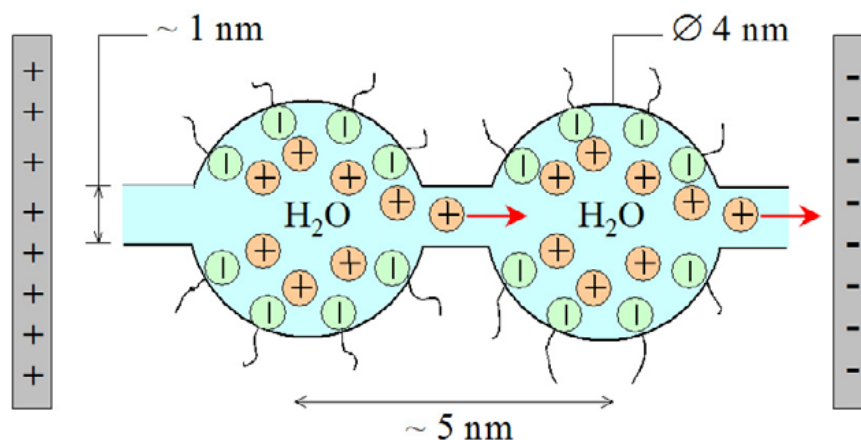


Figure 2.4 Ionic distribution of cluster network model [45].

On the other hand Nafion[®] derivatives are first synthesized by the copolymerization of tetrafluoroethylene (TFE) (the monomer in Teflon) and a derivative of a perfluoro (alkyl vinyl ether) with sulfonyl acid fluoride. The latter reagent can be prepared by the pyrolysis of its respective oxide or carboxylic acid to give the olefinated structure [45].

The resulting product is an $-SO_2F-$ containing thermoplastic that is extruded into films. Hot aqueous NaOH converts these sulfonyl fluoride ($-SO_2F$) groups into sulfonate groups ($-SO_3^-Na^+$). This form of Nafion[®], referred to as the neutral or salt form, is finally converted to the acid form containing the sulfonic acid ($-SO_3H$) groups. Nafion[®] can be cast into thin films by heating in aqueous alcohol at 250 °C in an autoclave. By this process, Nafion[®] can be used to generate composite films, coat electrodes, or repair damaged membranes.[36]

2.2.3.3. Properties of Nafion[®]

The chemical structure of Nafion[®] with its stable Teflon[®] backbone with the acidic sulfonic groups gives its characteristics properties. While Teflon[®] is one of the most hydrophobic chemical substances known, Nafion[®] perfluorosulfonic is one of the most hydrophilic. It will absorb water and some polar solvents rapidly, even at room temperature, in amounts dependent upon the number of sulfonic acid groups.

Nafion[®] is highly conductive to cations, making it suitable for many membrane applications. On the other hand, it is selectively and highly permeable to water. The hydration degree directly affected by ion conductivity and morphology of Nafion[®]. Nafion[®] is highly conductive due to its structural property. When the membrane becomes hydrated, the

hydrogen ions in the third region become mobile by bonding to the water molecules and moving between successive sulfonic acid groups [46].

Advancements in durability and chemical stability mean that Nafion[®] membranes are more resistant to decomposition at higher temperatures than other membranes which means Nafion[®] can operate high temperatures up to 190 °C. Not only advancements but also Teflon backbone interlaced with the ionic sulfonate groups gave Nafion[®] that properties. Also Nafion[®] is thermally stable.

In terms of membrane materials, especially literature on proton conducting membranes is mostly revolving around Nafion[®] in spite of its well known limitations like high cost (~ 1000\$/m), low performance under low humidity and at high temperature conditions and high fuel crossover [47,48]. Above all, its preparation involves environmentally nonfriendly fluorine based technology. In addition, chemical degradation in a fuel cell environment is also an issue of great concern for its reliability in long term operations. As the membranes become thinner, fluoride ions are detected in product water [49, 50]. Hence, there is a clear need for opting to alternative membrane materials which can overcome the major drawbacks of Nafion[®].

Nafion[®] is chemically resistive, but only alkali metals particularly sodium can degrade Nafion[®] under normal temperatures and pressures according to manufacturers' information.

While Teflon chemically inert, Nafion[®] membrane reacts with organic and inorganic bases. However, the sulfonic acid groups in the Nafion[®] are essentially immobile and immersed in a fluoropolymer matrix. Consequently, membranes can contact the skin without producing irritation.

Nafion[®] has acidity greater than that of 100% so it named as a super-acid catalyst which means sulfuric acid. The combination of fluorinated backbone, sulfonic acid groups, and the stabilizing effect of the polymer matrix make Nafion[®] a very strong acid, with $pK_a \sim -6$. [51] In this respect Nafion[®] resembles the trifluoromethanesulfonic acid, CF_3SO_3H , although Nafion[®] is a weaker acid by at least three orders of magnitude.

With the aim of modifying Nafion[®] meet specific characteristics various modifications can be made to a basic homogeneous membrane. For instance, in order to improve mechanical strength of heterogeneous membrane to the membrane weave fabric and surface treatment can be done in order to improve permselectivity.

2.2.3.4. Applications

Among broad application areas of Nafion[®], fuel cells, electrochemical devices, chlor-alkali production, metal-ion recovery, water electrolysis, plating, surface treatment of metals, batteries, sensors, actuators, Donnan dialysis cells, drug release, gas drying or humidification, and super-acid catalysis for the production of fine chemicals are the most common ones because of the polymer's superior properties [20][21][52].

In addition to their well-known applications in organic transformations they also a patent literature search reveal numerous applications in various electrochemical processes. In more recent years, the potential use of these materials as active or critical components in various devices has been explored.

Nafion[®] is also often cited for theoretical potential which means untested in a number of various fields. With consideration of Nafion[®]'s wide functionality, application as an actuator or sensor is the most significant one.

Nafion[®] has found use in the production of sensors, which application in ion-selective, metallicized, optical and biosensors. For chemical sensing, optically clear blends of poly(vinyl alcohol) and Nafion[®] applied as thin films to multiple internal reflection and spectroelectrochemical devices as surface modifiers. Also Nafion[®] catalyst filter modified carbon monoxide gas sensor for elimination of ethanol interference without compromising CO detection sensitivity [53,54]

On the other hand, biological compatibility makes Nafion[®] especially interesting. Nafion[®] has been shown to be stable in cell cultures as well as in the human body, and there is significant research for the production of higher sensitivity glucose sensors. [20]

In addition to all of the application areas mentioned above IPMCs show great potential as soft robotic actuators, artificial muscles and dynamic sensors in the micro-to-macro size range.

2.3. Actuation mechanism in IPMC

2.3.1. Description of the mechanism

The actuation mechanism of an IPMC actuator is known as bending. Briefly, the bending mechanism of IPMC involves a movement of hydrated metal cations to negative electrode (cathode), causing a volume difference between two electrodes of the IPMC strip.

As a matter of fact that, actuation of IPMC is a kind of electrochemical process known as electro-osmosis, which is also called electroendosmosis.

In 1809, F.F. Reuss was first described electro-osmosis, and this mechanism has growing applications in microfluidics. Generally electro-osmosis is the motion of polar liquid through a membrane or other porous structure caused by the action of an electric field, usually such a field generated by two electrodes, along charged surfaces of any shape and also through non-macroporous materials which have ionic sites and allow for water uptake, the latter sometimes referred to as "chemical porosity"[44].

In IPMC case electro osmosis caused by the migration with hydrophilic cation movement toward the anode between two platinum electrodes under applied electric potential. Therefore, IPMC bends. Here the movement of cation is electro-osmotic flow (EOF). For the most part electro-osmotic flow is the motion of ions in a solvent environment through very narrow channels, where an applied potential across the channels cause the ion migration. In IPMC solvent is the polar one, deionized water and very narrow channels are cluster network channels as mentioned previous part. By the way electroosmotic flow can occur in natural unfiltered water, as well as buffered solutions [55].

When subjected to an electric field, metal cations in the polymer membrane move towards the negative electrode, carrying with them bound water molecules. This ion-water flux causes a volume difference between two sides of the IPMC strip, producing a bending motion of the composite film towards the anode. Therefore, the capability and capacity of the migration of hydrated metal cations are important aspects of the IPMC performance.

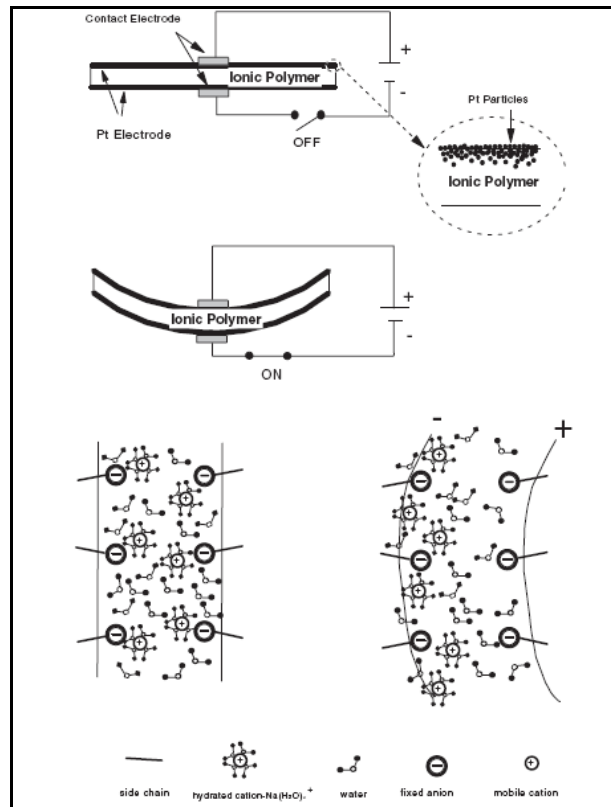


Figure 2.5 A schematic diagrams of the typical IPMC actuator and its actuation principle [41].

There are several different methods of approaches, in order to explain actuation mechanism of IPMC membrane. Both structure and transportation mechanism of ion exchange membranes bring about actuation of IPMC, a cluster network model, has been introduced by Gierke and Hsu [56, 57]. It also verified many times by several researchers Small-angle x-ray scattering by Roche et. al.[58] and TEM analysis Xue et. al. [59, 60], James et. al. [61]. In Nafion[®] fixed ionic groups located at the end of side-chains so can placed in their preferred orientation to some extent when membrane hydrated this different behavior of structure to water cause to form hydrophilic nano-channels, in other words interconnected cluster network. In addition to hydration when the electric field applied on the membrane, unbound cations can move through cluster networks towards the cathode, which is introduced by Nemat-Nasser this transport occurs at ionic rich places at the sides of the IPMC membrane. Depletion of cations near the anode formed a thin anodic layer while accumulation of cations near cathode formed thin cathode boundary layer. Although this accumulation cause local electrical imbalance, changes in the electrostatic forces and osmotic pressures the overall electric charge neutrality stay same. These changes also change the structural volume of the membrane and the response of the membrane by means of resting elastic resistance of

polymer matrix produce macroscopic deformation of IPMC membrane known as bending [62].

2.3.2. Enhancement of Actuation Performance

As documented in the relevant literature, two major approaches have been employed that increase the operation period of Nafion[®]-based IPMCs. In the first approach, a more durable inner solution was investigated for a replacement of the aforementioned water. Bennett and Leo examined the use of 1-ethyl-3-methylimidazolium trifloromethanesulfonate ionic liquid as an inner solvent for Nafion[®]-based IPMCs [63]. As reported, the advantages of ionic liquids, compared to water, have been identified as (i) superior stability and (ii) no risk of electrolytic decomposition. However, these benefits come with a loss of response speed, making the response speed much lower than that of conventional IPMC containing water.

In another study, Nasser investigated the use of ethylene glycol or glycerol, having high electrolytic stability, as an inner solvent for IPMCs [64, 65]. They found that the rate of response of IPMCs is low compared to water-containing IPMCs, due to the large size and high viscosity of these solvents.

In a second approach, an IPMC is given a protective surface coating in order to prevent the loss of water. Cohen and Leary reported that an effective barrier coating extended the operation period from a few minutes to many months [66], but they also found that the presence of the additional barrier layer on IPMCs could negatively affect the deformation because of the increased stiffness. Moreover, there is always a problem concerning the delamination of the protective polymer layer. Shahinpoor and Kim demonstrated that the blocking force of IPMCs was significantly enhanced by using a dispersing agent in the reduction process, which enabled the formation of fine Pt polycrystals on the surface and increased the depth of Pt penetration [67].

Another method is to increase the thickness of the IPMC strip. Optimization of this layer is crucial, as greater thicknesses yield greater surface conductivity which is essential in charging the membrane and enhance actuation. However greater metal thicknesses increase the composite's stiffness, increasing the force required for the same displacement. It was reported that an IPMC with a 2mm. thickness exhibited a blocking force of 20 gf under an electric potential of 6V [68, 69].

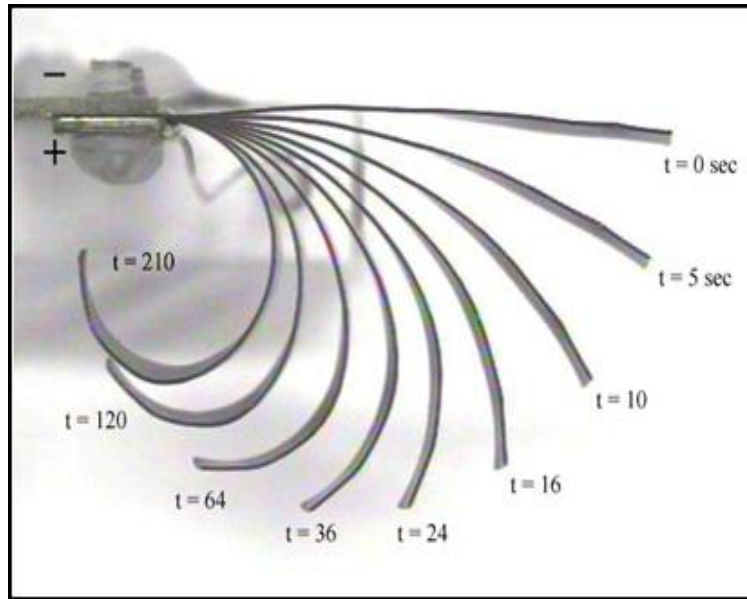


Figure 2.6 Actuation of typical IPMC under an applied voltage varied with time [70].

2.3.3. Factors affecting actuation

IPMC actuators' electrical-chemical-mechanical response is dependent various parameters. Most known and worked ones are described above.

As a matter of fact, there are two main factors that effect bending. These are the magnitude and the frequency of applied electric field.

As magnitude of the electric field increases displacement of IPMC strip increase so magnitude of electric field directly proportional with the displacement. In addition to that IPMC strips can be actuated by voltages between 1 and 5V. Ideal processing voltage values are up to 1.23V. Because voltages larger than 1.23V cause the hydrolysis of polar solvent by means of decreasing the performance of the actuator by forming bubbles on each side of the actuator. Meanwhile if surface resistance of the actuator reduced, performance would be increased. In addition, repeat number of Pt electroless plating increase conductivity of the electrodes so the actuation performance.

In recent years, extra deposition of silver or gold on Pt electrode has been also seen additive for IPMCs performance. In the mean time, as electrode thickness increases conductivity of electron increases however IPMC actuator becomes stiffer.

On the other hand frequency of electric field has inverse effect on displacement as frequency of electric field increases displacement of IPMC decreases. By the way increase of frequency, also increase bending response speed [70].

Not only electrode properties, but also polar solvent properties affect actuation performance. Especially amount of solvent migration, capability and capacity of the migration of hydrated metal cations have positive effect on actuation. In the meantime, redistribution of fixed ions and migration of mobile ions has an effect.

On the other hand the type of cations used, the nature and the amount of solvent uptake, the morphology of the electrodes, the composition of the backbone ionomer, the geometry and boundary conditions of the composite element, and the magnitude and spatial and temporal variations of the applied potential has an effect on actuation.

In addition to these main features contradiction and expansion of the outermost regions of a strip, geometric arrangement of composite layers and also characteristic properties such as modulus of hydrated polymer film, modulus of Pt and expansion coefficient of moisture are other features that affect actuation performance [71, 72, 73, and 74].

2.4.Types of predictive models for IPMC

Models for IPMCs are usually categorized as physical models, black box models, and gray box models [75].

2.4.1. Physical Models

Physical models are based on physics and chemistry, were first proposed by Shahinpoor [76] and Nemat-Nasser et al and Tadokoro [77, 78]. The most important property of that model is predicting behaviors of IPMCs quite accurately, but that model also has drawbacks such that the models require many assumed physical quantities that are nontrivial to be measured in experiments.

The first early physical model considers that electric field induced osmotic pressure as a dominant mechanism which is proposed by Shahinpoor in 1995[76]. However no solution was proposed for that model. Models which have both solution and compared experimental results were proposed late 2000.

In addition to these Tadokoro et al. [79] presented a new model for ionic polymer actuators. According to that model electric field application causes the mobile cations to migrate quickly across the thickness of the actuator from the anode (positive electrode) to the cathode (negative electrode), dragging water molecules along with them. That change due to water concentration also cause volume difference which is, decrease at the anode and an

increase at the cathode, causes contraction and expansion of the respective portions of the base polymer and induces a curvature in the actuator. That model called 'white box'. Also that model lay down that when the actuation signal is applied, there is a rapid bending toward the negative electrode continues with that on a slower time scale, osmotic pressure causes the water to diffuse in such a manner that the concentration is equalized across the thickness, resulting in a slow relaxation from the large curvature that was initially induced. The fast processes are probably cation and solvent motion, electrostatic stiffness changes, polymer conformation, and solvent orientation related, while the slow process is probably solvent diffusing backward to equalize pressure through the material and called back relaxation.

Another model was presented by Nemat-Nasser and Li, called the micromechanics model [80]. They also proposed a redistribution of the cations under application of an electric field, but with a difference from Tadokoro et al. Central to the micromechanics model is the idea that the sidechains of the polymer form clusters, which are saturated by water when the polymer is hydrated. Under the application of an electric field, the cations are redistributed, migrating towards the cathode. A locally imbalanced net charge density results and the associated electrostatic forces produce stresses that act on the polymer backbone, resulting in an electrically induced curvature of the actuator. Note that model is directly opposite those of Tadokoro et al., yet both models agree with experimental data.

In the white-box model, the electrostatic forces are secondary and cause bending towards the cathode. In the model presented by Nemet-Nasser and Li, the electrostatic forces are dominant and cause bending towards the anode. Nemet-Nasser and Li also considered sensing with ionic polymer transducers. They proposed that the displacement of the polymer causes a differential displacement of the effective charge centers of the anions and cations of each cluster. This differential displacement results in an electric potential across the transducer. Again, the simulated results compared well with an experiment.

In a later paper, Nemat-Nasser [81, 82] revised the 'cluster model' and focused only on the micro-mechanics he proposed are responsible for actuation. Unlike the previous work [80], he reported observing a slow relaxation towards the cathode after the initial motion towards the anode when a step voltage is applied to an actuator operated in air. The revised model is still based on the cluster morphology and the redistribution of cations under the application of an electric field. However, it also includes the effects of the hydration level and the water migration caused by the cation redistribution, factors not considered in the previous model.

Even with these factors considered, Nemat-Nasser still reasoned that ionic polymer actuator motion is due predominantly to electrostatic forces. He also concluded that all of the critical processes responsible for actuation occur within boundary layers that form at the anode and cathode when an electric field is applied. He credited the relaxation to a slow redistribution of the cations in the cathode boundary layer.

One difficulty with physical modeling of ionic polymer transducers is that the chemical and/or physical mechanisms responsible for the electromechanical transduction have not been conclusively identified. Also, the material parameters that appear in many of the proposed equations are not well known and do not lend themselves to direct measurement. These statements are strongly supported by the fact that the detailed physical models proposed by Tadokoro et al. [79] and Nemat-Nasser and Li [80, 81, 82] do not agree on the role of the actuation mechanisms, yet they both compare well to experiments.

Another issue with the physical models is that the governing equations are quite complex. These models will most likely prove useful in identifying and understanding the mechanisms responsible for transduction; however, much simpler models are needed for engineering design.

Unless different strategies have been proposed to describe the working principle of IPMC transducers with models on the other hand, are generally either too complex to be used in practical applications or too simple to guarantee sufficiently accurate predictions.

2.4.2. Black-box Models

Black box models, presented by Kanno et al [83] and Xiao et al [84], are convenient and are able to estimate curvatures and actuation displacements of IPMCs; however, they are only applicable to specific shapes and boundary conditions from which the models are empirically extracted.

The first black box model of ionic polymer transducer actuation was presented by Kano et al. [83]. The lack of a linear relationship suggests that ionic polymer actuator behavior cannot be modeled using a linear, time-invariant system, at least in the input range considered. However, it may also be a result of the inconsistent step response behavior observed by the Kano and other researchers [83, 85]. On the other hand, the nonlinear relationship between the constants and the input level was not discussed by Kanno et al.

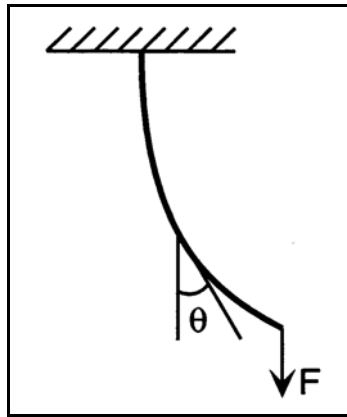


Figure 2.7 Bending principle and angle of IPMC [86].

Another black box model for cantilevered ionic polymer benders was put forth by Xiao and Bhattacharya [86].

While the black box models are relatively easy to understand and use, their scope is limited as they cannot accommodate any changes in actuator dimensions.

2.4.3. Gray Box Models

An alternative to the complicated physical models and the simplistic black box models, which are not scalable, are gray box models. These models incorporate well understood and easily modeled physical laws and use empirically determined parameters to represent the processes that are more complex and/or not well understood.

Also the grey box approach represents a useful choice and it is based on a set of simple equations that describe understood phenomena. These equations are ruled by parameters that are determined by processing experimental data. Provided that such parameters refer to macroscopic properties of the materials, the grey box approach can assure sufficiently general models to be used in design.

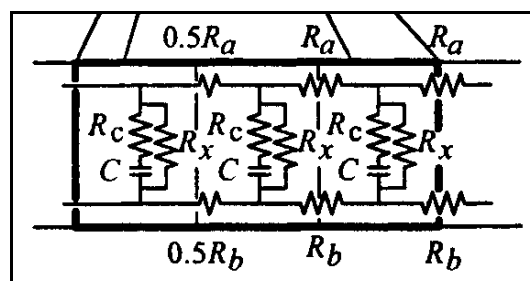


Figure 2.8 Equivalent circuit for the gray box model presented by Kanno et al [79]

The first and most widely accepted gray box actuator model was presented by Kanno et al. [79]. They represented the ionic polymer actuator using three stages that were connected in series, an electrical stage, a stress-generation stage, and a mechanical stage. For the electrical stage, the actuator was broken into discrete, one mm. long elements along its length. For the stress-generation and elastic stages, it was further subdivided into three layers through its thickness. In the electrical stage, each set of elements along the length was modeled using the equivalent circuit shown in Figure 2.8. The input of the electrical stage was the applied voltage and the output was current. This current was used as an input to the stress-generation stage, the behavior of which was governed by the relation

The mechanical stage consisted of a dynamic finite element model with proportional damping. The model was validated by comparing simulated and experimental results of the tip displacement with a step voltage input for a cantilevered bender. No verification of the model's scalability was presented. Note that this approach only accounts for the effect of the electrical response on the mechanical motion it does not allow the mechanical motion to affect the electrical response. The bidirectional energy conversion must be represented if a model is to be used for both sensing and actuation.

DeGennes et al. proposed another linear gray box model for the static case. This model is based on the premise that the water dragged by the migrating ions is responsible for the induced curvature. Although this model has a form that is conducive to developing a coupled actuator model for the material, it was only proposed as a steady-state model and is unable to represent any dynamics due to base polymer of the actuator. In addition, the water transport phenomenon described by the equations has not yet been conclusively linked to ionic polymer behavior. Lastly, no comparison to experimental data was published. [87]

2.5. Pros and Cons for IPMCs

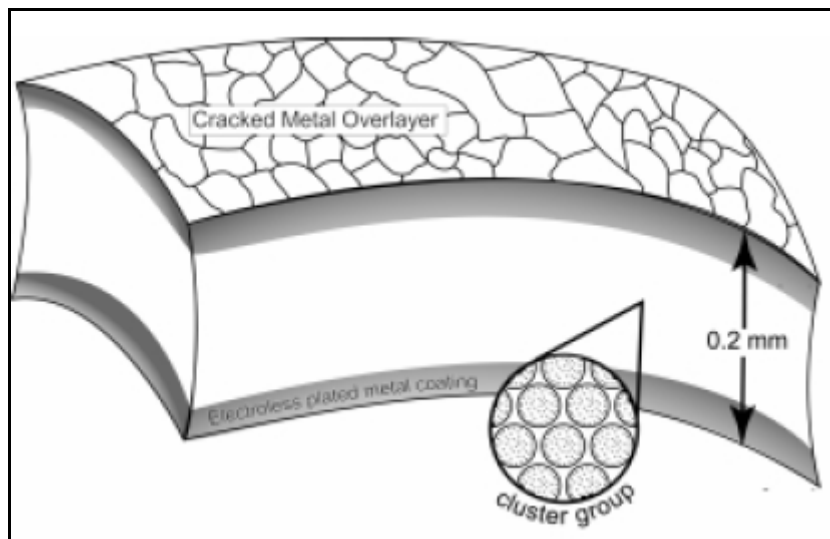


Figure 2.9 Typical IPMC actuator [88].

Typically, an IPMC is manufactured as a thin strip of soft ionic polymer, coated with metal electrodes, which bends with approximately constant curvature when voltage is applied to it. Because it has no moving parts, an IPMC is silent, and because it is polymer-based, it is lightweight and can be cut out easily in any shape. The ionic polymer metal composite (IPMC) is one type of electro-active materials with the characteristics of low electric driving potential, large deformation and aquatic manipulation.

One of the main characteristics is their softness. In addition to their softness vary according to fabrication techniques. IPMC hold promise as artificial muscles for the fields of bio-medical engineering and biologically inspired robotics. Also for bio-mimetic robotics softness provides a means to achieve curved body or limb shapes without the need of a large number of independently controlled actuators and joints. By the way they also provide a compliant interface to the environment so the biological compatibility of IPMC actuator is excellent [88], and thus it is appropriate for detecting or actuating in the human body. Because of that reason in recent years they are highly attractive to biomedical applications as an actuator or a sensor.

It is well known that all commercially available (asreceived) perfluorinated ion exchange polymers are in hydrogen ion form, semi-crystalline and may contain ionic clusters. The membrane form of these polymers has a typical thickness in the range of approximately 50–300 μm . Thinner commercial membranes permit fast mass transfer for use in various chemical processes.

Also knowing that such commercially available semicrystalline membranes are not melt-processable, they are not suitable for the fabrication of three-dimensional electroactive materials or other composite forms. Recent improvements show that newly developed fabrication method that can scale up or down the IPMC artificial muscles in a strip size of micro- to centimetre thickness. By carefully evaporating solvents out of the solution, recast ion exchange membranes were obtained [89]. With this method a number of samples having a thickness greater than 2 mm was fabricated with forces much greater than 20 gmf with a few millimetre displacements also IPMCs having a three-dimensional shape.

Beside their lightweight, low power consumption, compact design, fast response, noiseless motion and stability (it has no moving parts), they can also actuate under low operating voltages (1-5 V), display large bending deformation and operate both in air and wet conditions.

Because of their polymer-based structure, they are not only flexible but also can be cut out easily in any shape [90, 92].

Beside their numerous advantages conventional Nafion[®]-based IPMCs have the major drawbacks of a short operation time in dry operation environment due to the loss of inner solution either by natural evaporation because of that reason they need of staying the humid in dry conditions. And leakage due to surface expansion or electrolysis process occurring on the two electrode layers (at voltage as low as 1.23V in case of water), while the motion perpendicular to the main axis, the low driving voltage and the swollen status of the IPMC strip can only generate a limited value of blocking force (about mN).

However, the adhesion between polymer and electrode is a big problem during the fabrication of IPMC actuator. In order to solve this problem, the electroless plating method had been used to fabricate the electrode layer, but it needed complex pretreatment to roughen the surface of polymer with high cost and time-consuming.

IPMCs can be easily pre-formed or cast in any shape, including three dimensional shape. If the pre-shaped curve has segments with opposite curvature, on application of a voltage one side will open, while the other will close.

Several approaches have been reported to be effective for addressing these drawbacks of IPMCs. They are (i) optimization and additional treatment of electrode layer fabrication process; (ii) increasing IPMC thickness [30]; and (iii) using specific inner solution systems based on ionic liquid [93].

2.6. Applications of IPMCs

IPMCs are considered to be one of the most promising smart materials because they have light weight and can make large bending deformation under low driving voltages. Thus they are expected to be applied to soft robotic actuators and artificial muscles, as well as dynamic sensors in the micro-to-macro size range. Moreover, they can be used to make an embedded system, which provides great advantages for the integration of sensors and actuators. However, IPMCs generate low actuating force, which limits its application to actuators. Therefore, there are increasing demands to improve the performance of IPMCs in terms of the actuating force. The actuating force is related to the bending stiffness and the thickness of the ionic polymer membrane.

The electronic active polymer, IPMC, could be potentially used as the actuator of the active guide-wire, effective biomimetic sensor and artificial muscles. Ionic polymer metal composites (IPMC) exhibiting large bending deformations under a low electric field have recently attracted a great deal of interest in the fields of dynamic sensors, robotic actuators and artificial muscles due to advantages.

The major success of one research material directly proportional with how far is it applicable for potential applications. Unless IPMC could not take the advantage of driving frequency or force output in applications they have ultimate success where bending actuation, low operation voltage in other words low energy consumption, small and compact design, lack of moving parts and relative insensitivity to damage necessary.

Within the context of features mentioned above IPMCs have numerous potential applications using as sensors, actuators, artificial muscles, and transducers. Generally, IPMC s most critical applications are divided into two main groups. One of them is industrial applications and the other one is biomedical applications. By the way it is definitely obvious that the extent of application areas of IPMCs goes beyond the scope of that work. The breadth and the depth of all such applications of IPMCs as biomimetic robotic distributed sensors, actuators, transducers and artificial/synthetic muscles presented.

2.6.1. Mechanical grippers

Ordinary IPMC actuators can be used for numerous applications by means of using several different design techniques. For example if some actuators wired and sandwiched in a way such that they bend opposite directions so kind of mechanical tweezers can be fabricated.

With beginning with the tweezer example IPMC actuators may used as micro or macro gripper.

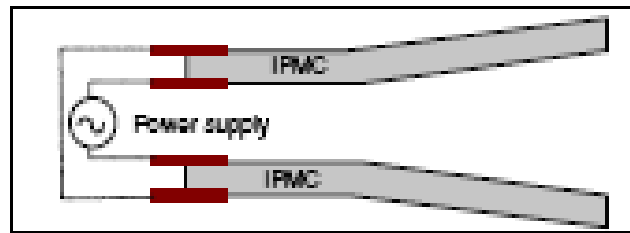


Figure 2.10 Example of multi finger gripper [94].

To date, multi-finger grippers that consist of two, four, and eight fingers have been produced, where the four-finger gripper was able to lift 10,3 g mass. This gripper prototype was mounted on a 5 mm diameter graphite/epoxycomposite rod to emulate a light weight robotic arm. This gripper was driven by a 5 V square wave signal at a frequency of 0.1 Hz to allow sufficient time to perform a desirable demonstration of the capability of the gripper (opening the gripper fingers, bringing the gripper near the collected object, closing the fingers and lifting an object with the arm). The demonstration of this gripper capability to lift a rock was intended to pave the way for a future potential application of the gripper to planetary sample collection tasks using an ultra-dexterous and versatile end-effector or to handle soft biological objectives.

At that point one question came by, what is the fascinating difference of IPMC grippers relative to conventional actuators. The answer is their intrinsic material softness. In addition to that property they are able to operate in harsh conditions such as 1 Torr of pressure and -140°C temperature so that is also a good reason of their application in space environment by NASA/JPL.

Also Viking and Mars Pathfinder missions indicate that operation on Mars involves an environment that causes accumulation of dust on hardware surfaces. The dust accumulation is a serious concern that hampers long-term operation of optical instruments due to loss of visibility and degrades the efficiency of solar cells to produce power.



Figure 2.11 Demonstration of IPMC wipers used by NASA/JPL[42].

To remove dust from surfaces one can use a similar mechanism as automobile windshield wipers. Contrary to conventional actuators, bending EAP has the ideal characteristics that are necessary to produce a simple, lightweight, low power wiper mechanism. Specifically, the IPMC responds to activation signals at a frequency of less than a Hertz with a bending angle that can exceed 90 degrees span each way depending on the polarity. Since an EAP wiper was demonstrated to remove dust effectively. [42, 94]

2.6.2. Robotic swimming structure

Also with different arrangement of the IPMC actuator showing an elastic construction with imprinted electrodes and advantage of showing relatively high performance in water than dry environment for use as a robotic swimming structure, more specifically a robotic fish.

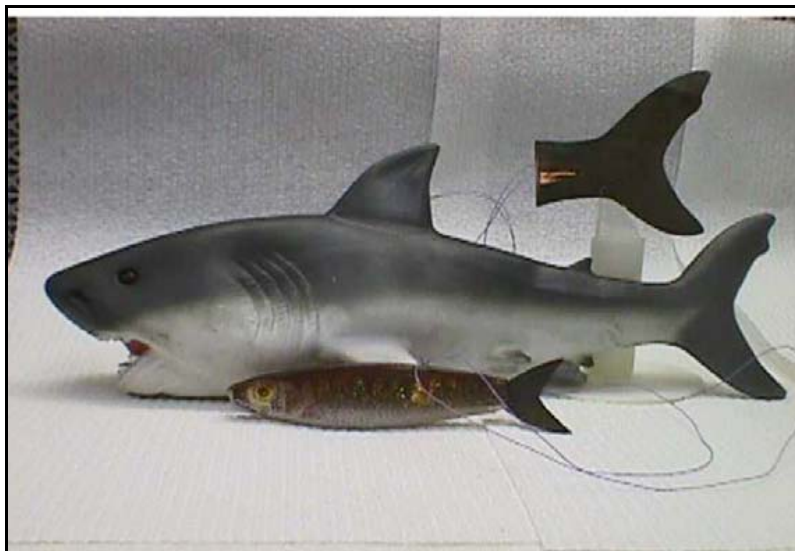


Figure 2.12 A designed and fabricated undulating caudal fin actuator and two robotic fish equipped with IPMC fin actuator [94].

These robotic swimming fishes and submarine structures fundamentally contain a sealed signal and powergenerating module (preferably in the head assembly) can be made to

swim at various depths by varying the buoyancy of the structure by conventional means. Beside this, remote commands via radio signals can then be sent to modulate propulsion speed and buoyancy. Based on such dynamic deformation design and observed characteristics, a noiseless swimming robotic structure was constructed and also tested for collective vibrational dynamics.

In order to actuate robotic submarine structures by means of energizing one pair (across) of actuators at a time and then the consequent pairs downstream, one can produce a propagating or traveling wave downstream on each side of the fish. This will produce a sting-ray type of motion which propels the swimming structure forward.

In addition to remotely controllable stealthy, noiseless, biomimetic swimming robotic fish made with IPMCs also electrically controllable caudal actuator fins (propulsion, and gross turning and maneuvering) and pectoral actuator fins (fine turning and maneuvering) were designed and laboratory-tested for naval applications[94, 95].

2.6.3. Composite wing flap

In order to accommodate several power specifications of air vehicles, IPMC actuators sandwiched together. In addition to that each independent actuator has difference in length. The reason of that is to provide different stiffness and resonant frequencies along the composite wing. With these differences in structure one can produced not only thicker but also more powerfull actuators tat can handle higher loads. Figure 2.13 shows the structure of composite wing flap made by IPMCs.

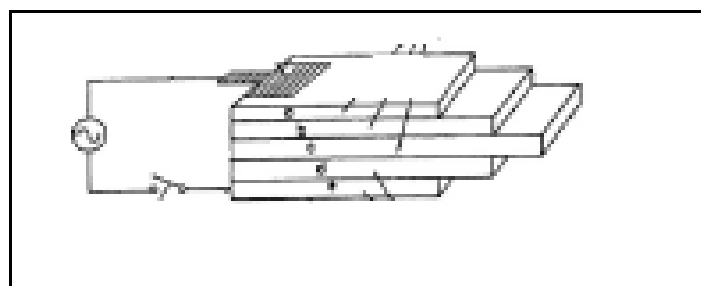


Figure 2.13 Schematic representation of composite wing flap [94].

Not only those stated above, but also linear actuators, three dimensional actuators, metering valves, diaphragm pumps made with IPMCs, microelectromechanical systems, electromechanical relay switches, continuous variable aperture mirrors and antenna dishes, musical instruments, resonant flying machines are industrial application areas of IPMC actuators [94].

2.6.4. Biomedical applications

Ionic polymer-metal composites (IPMCs) are a type of actuators, which due to their softness hold promise as artificial muscles for the fields of bio-medical engineering and biologically inspired robotics. Because the possibility of hard objects may damage biological tissue softness is advantageous for biomedical applications [96].



Figure 2.14 From biological muscles to artificial ones [97].

As a demonstration of the performance of the IPMC actuator from the proposed traditional method, therefore, we considered the application of IPMC actuators to emulate an artificial finger. A simple form of artificial finger was fabricated without any joints; one IPMC strip is used for a finger. To demonstrate the performance of the improved IPMC actuators, we fabricated an artificial finger with three joints using 5-film stacked IPMC actuators.

In addition to described applications they are also utilize for three-dimensional actuator, exo-skeletal human joint power augmentation, metering valves, IPMC contractile serpentine and slithering configurations, diaphragm pumps using flexing IPMC strips[94,97]

CHAPTER 3 MATERIALS AND MANUFACTURING

3.1. IPMC Materials

According to relevant literature and as mentioned in this work, Nafion[®] is the most important and common polymer membrane in production of IPMC actuators. Nafion[®] membranes were commercially purchased at different thicknesses from Sigma-Aldrich. They are in the hydrogen ion form. They have had 50, 90, and 180 μm . thickness values. After plating them by electrochemical planitization method their ticknesses rise to 70, 110 and 200 μm respectively and they were subjected to actuation experiments [98, 99].

3.2. Electroless plating

To date, many fabrication processes have been used for the preparation of ionic polymer metal composite (IPMC) membranes from conductive metals and perfluorosulfonic polymers such as Nafion[®].

Current state-of-the art IPMC actuator strips are commonly manufactured by following the process reported below [98]. It consists of two distinct preparation steps named initial compositing and surface electroding known as electrochemical platinization method also used in this thesis work. The method overall contains pretreatment, adsorption (ion-exchange) Process, primary plating (reduction) process, secondary plating (developing) process, ion-exchange processes.

The underlying principle of processing these novel IPMCs is first level preparation named as surface roughening and consists of four main steps; mild sandblasting, ultrasonic washing, treatment with HCl and treatment with water Nafion[®] membrane for platinum plating. Main reason of that step is preparing the Nafion[®] for plating.

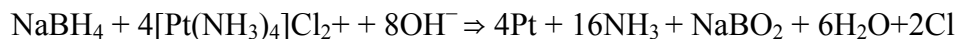
- a. Mild Sandblast: Sandblasting the surface of the membrane with using emery paper in order to increase the surface area. The type of the emery paper changes according to thickness of the polymer membrane. It has maximum granul size of 500C.
- b. Ultrasonic Washing: In order to remove the glass beads and residues by washing the membrane with water preferably using ultrasonic cleaner for 15 minutes without temperature application.

c. Treatment with HCl: Boil the membrane in dilute hydrochloric acid (HCl aq, 2 N solutions) for 30 minutes to remove impurities and ions in the membrane after that boiling rinse it with deionized water. The main idea of that boiling process is to develop depth of the pores which is obtained by emery paper.

d. Treatment with Water: Boil the membrane in deionized water for 30 minutes to remove acid and to swell the membrane. After that last pretreatment step the roughened membrane can be stored in deionized water.

The second level known as ion-exchange (adsorption) capability that physically loading of conductive primary powder layer into the ionic polymer network forms a dispersed particulate layer. This primary layer functions as a major conductive medium in the composite. Samples of these Nafion[®] membranes are immersed in a metal salt solution of Tetraamineplatinum(II) Chloride monohydrate (Pt(NH₃)₄)Cl₂ CAS 1393-33-0 in order to let platinum to diffuse in membrane. For that reason platinum complex (Pt (NH₃)₄)Cl₂ solution is prepared due to 2 mg Pt per ml. Then the membrane is immersed in that solution. By the way Pt amount in the solution depend on the surface area of the membrane to be plated. The solution should contain more than 3 mg of Pt per cm² membrane area. After immersing the membrane, 1 ml of ammonium hydroxide solution (5 %) is added to neutralize the platinum solution. At last, the membrane is kept in the solution at room temperature for more than 3 hours (one night usually).

Subsequently, loading of primary conductive powder layer of dispersed particles of a conductive material is further secured within the polymer network with smaller secondary particles via chemical plating, which uses reducing agents to load another phase of conductive particles within the first layer; another level called primary plating (reduction). The primary reaction for platinum composites is



By using appropriate reducing agent NaBH₄ for chemical reduction of the metal ions on to the surface of membrane forming thin layer of electrodes. As can be seen in Figure 3.1, the metallic platinum particles are not homogeneously formed across the membrane but concentrate predominantly near the interface boundaries.

In the primary plating process, 5 wt% aqueous solution of sodium borohydride is prepared. After rinsing the membrane with water, the membrane is placed in a water bath at 40°C. Note that, both amount of water and reducing agent should be proportional with membrane surface area. Then, 2 ml of the sodium borohydride solution (5 wt% NaBH₄ aq) is added every 30 min for 7 times. The amount of the reagent should be proportional to the area of the membrane. In the sequence of addition, the temperature is raised up to 60°C gradually. Then, 20 ml of the reducing agent is added and is stirred for 1.5 hr at 60°C. At the end of these processes, black layer of fine Pt particles deposits only on the surface of the membrane. At the end of that primary plating process the membrane is rinsed with water and immersed in dilute hydrochloric acid (0.1 N) for an hour.

The primary reason of this compositing process is to metalize inner parts of the membrane actuators by ion exchange of the protons H⁺ with metal cations (Pt⁺²). This initial compositing process requires an appropriate metal salt such as (Pt(NH₃)₄)Cl₂ in the context of chemical reduction processes. These processes are similar to those that are evaluated by a number of investigators including Takenaka et al [100] and Millet et al [20]. The principle of the compositing process is to metallize the inner surface of the polymer by a chemical-reduction means such as LiBH₄ or NaBH₄. After this exchange process Pt⁺² ions placed predominantly near the surfaces but overall dispersion is not homogeneous. In addition to the initial platinum layer formed by the initial compositing process also the roughened surface disappears. In general, the majority of platinum salts stay in the solution and precedes the reducing reactions and production of platinum metal [101].

The amount of platinum deposited by the Primary Plating (Reduction) process is only less than 0.9 mg/cm², which depends on the ion exchange capacity, thickness of the membrane and the structure of the Pt complex. Additional amount of platinum is plated by developing process on the deposited Pt layer. In the subsequent Secondary Plating (developing) Process, multiple reducing agents are introduced under optimized concentration to carry out the reducing reaction.

A 240 ml aqueous solution of the complex (Pt(NH₃)₄)Cl₂ containing 120 mg of Pt again amount of solution depend on surface area should be prepared and 5 ml of the 5% ammonium hydroxide solution should be added. Plating amount is determined by the content of Pt in the solution. A 5% aqueous solution of hydroxylamine hydrochloride (NH₂OH-HCl) and a 20% solution of hydrazine (NH₂NH₂) are also prepared. Pt solution is kept at 40°C and stirred the membrane placed in that Pt solution. After that 6 ml of the hydroxylamine hydrochloride solution and 3 ml of the hydrazine solution has added in every 30 minutes. In the sequence of

addition, the temperature is risen up to 60°C gradually for 4 hours, and gray metallic layers will form on the surface of the Nafion® membrane. At the end of this process, a small amount of the solution is sampled and boiled with the strong reducing agent (NaBH₄) to check the end point. By the way it is dangerous to add NaBH₄ powder in a hot solution, because of the gas explosion. So NaBH₄ solution is added to a cold solution, then, warmed the solution on a water bath. If any Pt ion remains in the plating solution, the color of the solution turns to black. In such cases, continue to develop Pt with addition of the NH₂OH-HCl and NH₂NH₂ solutions. If there is none of Pt ion in the chemical plating solution, the membrane rinsed with water, and boiled in dilute hydrochloric acid (0.1 N) to remove the ammonium cation in the membrane [102].

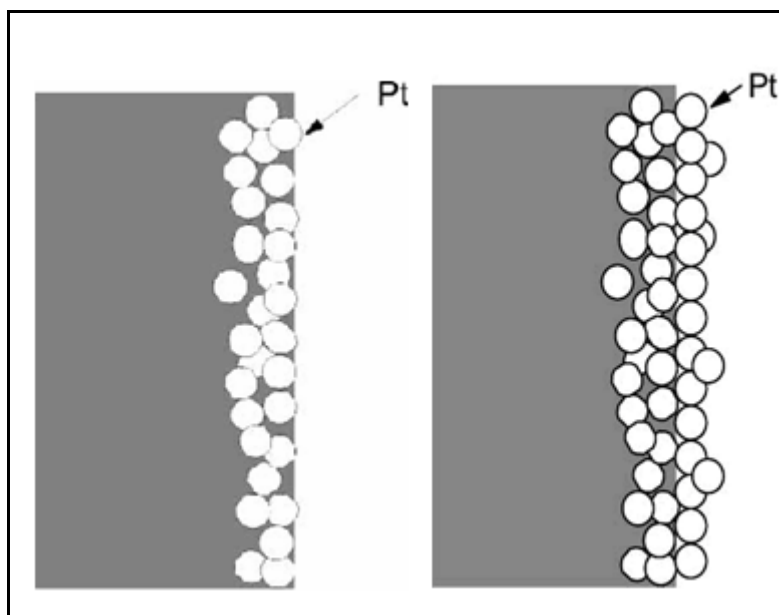


Figure 3.1 A schematic representation of IPMC after first and second plating processes [41].

In turn, both primary and secondary particles can be secured within the ionic polymer network and reduce the potential intrinsic contact resistances between large primary particles. Furthermore, electroplating can be applied to integrate the entire primary and secondary conductive phases and serve as another effective electrode.

Next, IPMC actuator is converted to H⁺ form by boiling the membrane in diluted HCl acid solution for an hour. After washing with water, H⁺ in the composite can be exchanged for any cation by immersing in a solution of the chloride salt of the cation. In my work, I used KCl salt solution in order to H⁺ ion exchange by immersing the membrane and kept for 3 days. In the literature it has shown that the cations like Na⁺, Li⁺ and K⁺ in the IPMC actuator generally exhibit better bending performance than other ions [41, 102].

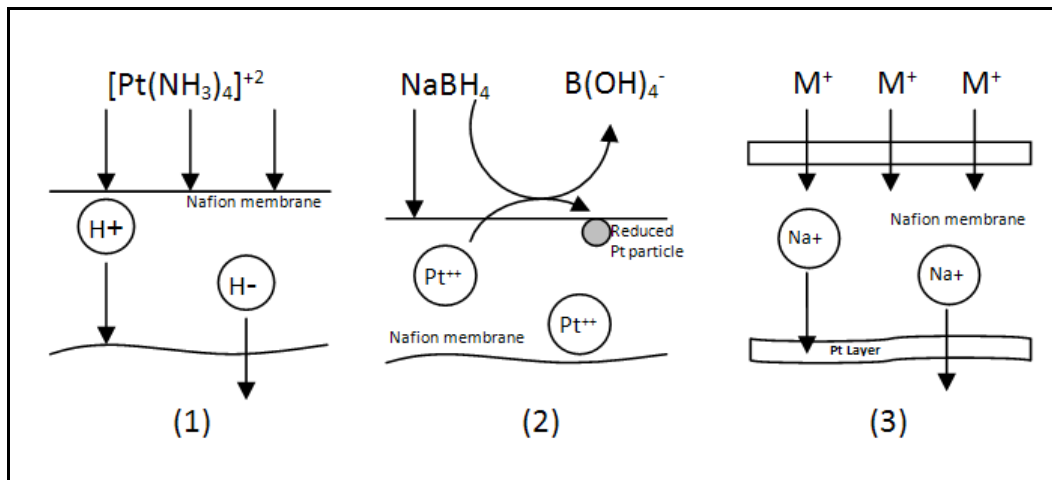


Figure 3.2 Scheme for IPMC fabrication: (1) ion exchange with noble metal salt; (2) reduction of metal at surface; (3) ion exchange with desired cation

The isolated Pt nanoparticles appear to be essential to the actuation of the IPMC that these conductive particles be dispersed through a finite depth of the membrane in order to increase the depth of the electrostatic double-layers, and hence the fraction of the material which experiences the electric field. It has been experimentally observed that the platinum particulate layer is buried microns deep (typically 1–20 μm) within the IPMC surface and is highly dispersed. Due to different preparation processes, morphologies of precipitated platinum are significantly different.

Platinum is the preferred metal because it is immune to corrosion over a larger range of electrochemical potential than other metals, and hence allows the use of higher driving voltages without damage.

The fabricated IPMCs can be optimized to produce a maximum force density by changing multiple process parameters. These parameters include time-dependent concentrations of the salt and the reducing agents.

Although, the traditional fabrication process gave outstanding surface electrodes and excellent performance characteristics to IPMC membranes, there are several drawbacks of using that process. These are high cost due to the use of noble metals such as platinum, gold, palladium, etc. as an electrode material and time-consuming associated complex chemical processes. For IPMCs to be productively adopted as industrial actuators or sensors, one should be able to reduce their manufacturing cost significantly, simplify the compositing and also find alternative electroding processes.

Some of the effective fabrication techniques are described below;

3.3. Fabrication of solution recasted Nafion[®]

In order to prepare solution recasted Nafion[®] film sample, commercially available appropriate liquid Nafion[®] solution was purchased from DuPont. According to manufacturer's specification, known quantity of liquid Nafion[®] with an additive is placed in Teflon[®] coated Pyrex glass. Then, annealing is performed at an elevated temperature of 70° C then temperature raised at 150°C for further curing. At last platinum electroding is done on both sides of the sample as indicated traditional electroless plating. The advantage of this method is that provides an availability of producing thicker Nafion[®] sheets. However, this method requires delicate tuning of process variables such as temperature and concentration of specific solvent, and it thus has a reproducibility problem. In addition to that during solvent evaporation the solidified Nafion[®] may develop surface cracks [103, 104].

3.4. Other potential techniques

Although not implemented in this work, this section describes other techniques that can be used in IPMC making for completeness.

The method in order to control the thickness of the IPMC is hot pressing method. In this method the Nafion[®] films tailored in proper dimensions, rinsed with acetone, and stacked in the stainless steel mold with polyimide film. Then the mold is placed and preheated, to 180°C, and hold without pressure for 20 min, then pressed with 50 MPa at 180°C for 10 min. After that it is allowed to cool down to the ambient temperature in the air and the film is boiled in 3 wt % sulfuric acid at 70°C for 1 h, in 10 wt% hydrogen peroxide at 70°C for 1 h, and in deionized water for 30 min.

The advantage of hot pressing method is not only to control thickness variation but also the simplicity, repeatability and yields thick IPMC actuators with higher stiffness than the solution casting method [105].

Traditionally the membranes are either extruded from dry polymer or cast from polymer solutions in appropriate solvents. Recently, another approach for fabricating membranes and catalyst layers has been proposed that is based upon electrostatic polymer processing, namely electrospraying and electrospinning.

In that new method, a solution of Nafion[®] in a mixture of lower aliphatic alcohols and water (Sigma-Aldrich) is electrosprayed from a syringe using a blunted needle and an applied voltage of 20 kV and approximately 5ml of solution delivered at a rate of 2 ml/h. This solution is deposited onto a rotating Teflon-coated mandrel which remained grounded at all times. With that method films with thicknesses of approximately 50–60 μm produced [106].

One other method to improve physical properties of polymer without sacrificing other important ones is fabrication of multilayered Nafion[®]/MMT and Nafion[®]/silica nanocomposites IPMC actuators.

A considered amount of montmorillonite (3, 5, and 7 wt. %) or silica (5 and 10 wt. %) is added into the Nafion[®] solution and mixed. And then, the mixture is poured into a Teflon mold and dried in a vacuum oven in order to obtain a thin nanocomposite film with a desired thickness. After that, by increasing the temperature to 140 °C for 2 h. an annealing step is performed with the purpose of advance the mechanical properties of the solvent cast Nafion[®] film and its intactness in water.

The advantages of using a Nafion[®] nanocomposite may be two-fold: (i) the stiffness of the polymer matrix can be increased, producing a larger blocking force of the IPMC and (ii) other important features of IPMC can be altered in a favorable manner. Additionally, fumed silica can be acidified and neutralized to introduce additional metal cations to the IPMC, which may exhibit an improved performance in terms of displacement and blocking force [107,108].

After all these different Nafion[®] membrane fabrication methods not only different thickness one but also additive contained IPMCs are prepared with using a wellknown electroless plating method.

As indicated in actuation mechanism, in order for the transduction to occur in Nafion[®] membranes, the cations within the membrane must be dissociated by saturation with an appropriate solvent. Typically, the solvent used has been water. Although water is the most usefull solvent, it has some drawbacks such as volatility, leading to dehydration and the corresponding loss in performance of these actuators when operated in air [109]. For that reason researchers are trying to find alternative ionic solvents. For instance the hydration problem can be overcome by using ionic liquids as the solvent in these actuators. Ionic liquids offer increased environmental stability and a larger electrical operation window compared to water but suffer from high viscosity. On the other hand actuators solvated with ionic liquids have slower strain rates compared to water hydrated samples. This new ‘direct assembly

fabrication' method allows the use of large surface area metal powders to increase the electrode/polymer interface.

The electric double layer capacitance increases linearly with the interfacial area, and therefore increasing the metal powder content in the electrode increases the performance of the actuator. Furthermore, the conductivity through the electrode is also proved to be critical to the speed of the actuation mechanism in ionic polymer transducers.

Not only these described above but also other methods like hot-embossing, electroplating and polymer coating, etc. They were provided for the adhesion promotion in decreasing the cost and time during fabrication [110, 111].

Also, there are still some problems during the fabrication of IPMC, such as the inability to stay humid, and the difficulty of avoiding electrolysis at higher applied driving voltage (>1.23 V) [42,112]

CHAPTER 4 EXPERIMENTAL METHODS

4.1. Unblocked Tip Displacement Experiments

During this study, several test specimens have been prepared especially based on their geometry by electrochemical platinization method. Main IPMC actuator specimens that used in tests have rectangular shape with dimensions of 50mm long and 5mm wide. They were clamped at one end and kept free at the other. The actuators are fixed vertically on 5mm from the edge and submersed into water filled aquarium having length 15x7x5 cm.

In this case the experiment medium is the deionized water. The specimen is subjected to electrical load by arbitrary waveform generator (Agilent 33120A). This load is a kind of sinusoidal wave with small magnitude which means 1-5V applied. On the other hand, applied electrical load is described peak to peak. That means 2V and -2V values applied at the same time to different sides.

Movements and displacements when the specimen is subjected to electrical load were recorded by a video camera (Sony CDR-SR32E). Once the actuation experiment and recording is done, the displacement is measured using freeware image processing software: WinDIG 2.0 as shown in Figure 4.1.

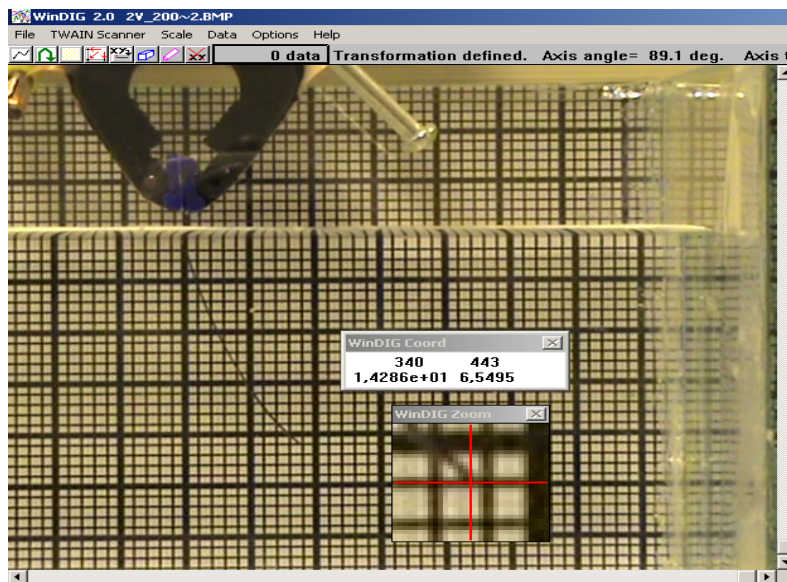


Figure 4.1 Interface of the image processing software

In our work, experiments were carried out for each of the three actuators namely 70, 110, and 200 μm thick flat IPMC actuators at quasi-static excitation voltage of 0,5, 1, 1,5 and 2V. The combinations of the thickness and voltage resulted 12 test points.

At each test point tip displacement measurements were repeated 3 times. Averages of the three measurements at each test point were then considered as the result of the associated combination of thickness and applied voltage.

4.2. Blocking Force Experiments

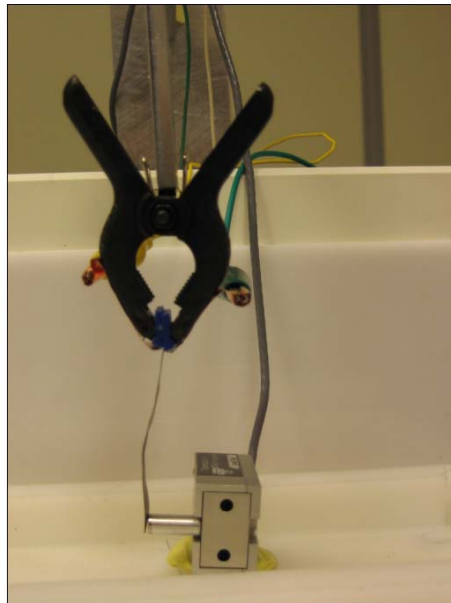


Figure 4.2 Experimental setup of Blocking Force.

To calculate the “equivalent” young’s modulus of IPMC strip, blocking force should be measured. We measured the blocking force values for the specimen having thickness $200\mu\text{m}$ with force transducer (Transducer Techniques, DPM-3, 10gr.) while excited at 2 volt and minimum frequency (10 mHz).

CHAPTER 5 COMPUTATIONAL METHODS

5.1. Equivalent bimorph beam model

In this thesis work, IPMC actuators are treated as the equivalent bimorph beam model to predict the performance of the actuators and to obtain the electro-mechanical coupling coefficient and young's modulus which can be considered as "equivalent" material parameters for finite element analyses.

The equivalent beam model and an equivalent bimorph beam model are presented as gray box models. The main issue of our work equivalent bimorph beam model combined with two important physical properties of IPMCs: young's modulus, elastic modulus and electro-mechanical coupling coefficient, d_{31} . These physical quantities are determined by both using outputs of experiments and the equivalent bimorph beam model equations for load and displacement.

When equivalent bimorph beam model is used with physical properties, almost perfect correlation is obtained. After physical properties are obtained, these properties can be used with finite element analysis (FEA) to simulate the IPMC actuation. Further, effective designs can be introduced with finite element analyses.

In the equivalent bimorph beam model, shown in Figure 5.1, it can be assumed that an IPMC has two virtual layers that have the same thickness (each is the half the thickness of the actuator). Under an imposed electric field across the material, the upper layer and the lower layer of an IPMC expand or contract, opposing each other, to produce the IPMC's bending motion [88]. Generally, for a cantilevered bimorph beam with a sandwiched elastic layer, the tip displacement, s , and the blocking force, F_{bl} , can be written as follows;

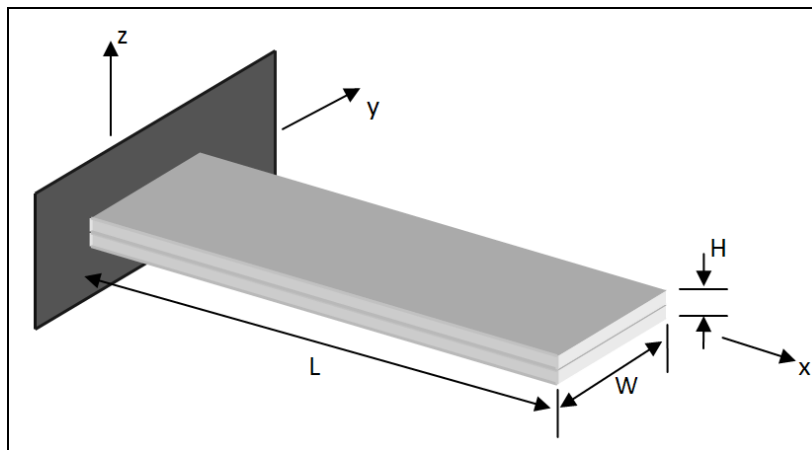


Figure 5.1 Equivalent bimorph beam model

It is assumed that IPMC has two layers having the same thickness. The reason of modeling the IPMC as two layers is to produce IPMC's bending motion. Bending motion is created under an applied electric field due to opposing motion of layers in other words while one layer expands, the other layer contracts.

Generally, for a cantilevered bimorph beam with a sandwiched elastic layer, the tip displacement, s , is given by [88],

$$s = \frac{3L^2}{2H} \frac{(1+b)(2b+1)}{ab^3 + 3b^2 + 3b + 1} d_{31} E_3 \quad (5.1)$$

And the blocking force, F_{bl} , can be written as follows [88];

$$F_{bl} = \frac{3WH^2 E}{8L} \frac{2b+1}{(b+1)^2} d_{31} E_3 \quad (5.2)$$

where a and b are the young's modulus ratio and the thickness ratio, respectively, of the sandwiched elastic layer and the outer layers, E_3 is the electric field, and d_{31} is the electro-mechanical coupling coefficient in which the subscripts 1 and 3 stand for the x-direction and the z-direction, respectively. In our assumption for an IPMC actuator, there is no sandwiched elastic layer, therefore the ratios are zeros ($a = b = 0$). From equation (5.1), a relationship between the input voltage, $V (=HE_3)$, and the induced tip displacement, s , of an IPMC based on an equivalent bimorph beam model given by:

$$s = \frac{3d_{31}VL^2}{2H^2} \quad (5.3)$$

where d_{31} equivalent or effective electro-mechanical coupling coefficient in which the subscripts 1 and 3 stand for the x-direction and the z-direction, respectively, V is the applied voltage, L is the length of the beam, and H is the thickness of the beam.

By manipulating the Eq. 5.3 effective coupling coefficient d_{31} can be written as:

$$d_{31} = \frac{2sH^2}{3VL^2} \quad (5.4)$$

By using the tip displacement values obtained from clamped-free IPMC actuator tests, the electro-mechanical coupling coefficient can be calculated from Eq. 5.4. This electro-mechanical coupling coefficient is an essential component in this study as it enables use of commercial finite element software in simulating the IPMC behavior when excited.

On another note, in the equivalent bimorph beam model, the young's modulus, E , contributing to the bending stiffness of an IPMC is determined by using the blocking force

equation (5.2). Disregarding the sandwiched elastic layer, a relationship between the input voltage, V ($=HE3$), and the blocking force,

F_{bl} , of a cantilevered IPMC actuator can be written as follows [88];

$$F_{bl} = \frac{3WHEd_{31}}{8L} \quad (5.5)$$

In order to determine the equivalent of Young's modulus, equation (5.3) is rewritten as follows[88];

$$E = \frac{8LF_{bl}}{3WHd_{31}V} \quad (5.6)$$

5.2. Finite element analyses

MD.NASTRAN is closely linked with the pre- and postprocessing of MSC.Patran, offering a completely integrated environment for modeling and analysis. A wide range of third-party pre and postprocessors, solid modelers, and CAD programs also offer direct interfaces to MD.NASTRAN. The result is unmatched flexibility, integrating MD.NASTRAN into an existing design environment.

MSC.PATRAN was used for modeling and post-processing the results from MD.NASTRAN when used as a solver. Since equivalent bimorph beam model is the reference, IPMC strip was modeled as a bi-layer plate. IPMC strip was modeled with 4-node QUAD elements having 1mm edge length.

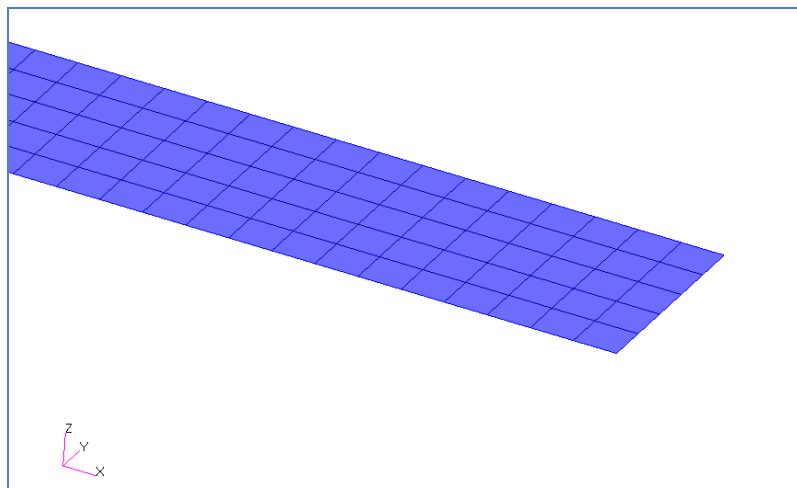


Figure 5.2 Finite element model of IPMC

Since MD.NASTRAN lacks of capability for performing coupled electro-mechanical coupled analyses, MD.NASTRAN requires an analogous thermo-mechanical analysis. Using thermal analogy technique, by using equation experimentally calculated 'effective electro-

mechanical coupling coefficients' were converted into coefficient of thermal expansion α as follows [88];

$$\alpha = \frac{d_{31}}{H/2} \tag{5.7}$$

Since an IPMC can be assumed to have two virtual layers in the equivalent bimorph beam model, as shown in Figure 5.1, the thickness, t , is defined as $H/2$. The electric potential applied across a virtual layer is half of the total voltage that is applied across the total thickness of an IPMC.

To model the IPMC as two layers, two isotropic materials were defined with the same material properties. However, one is having positive equivalent coefficient of thermal expansion, whereas, the other one is having the negative. By doing so, under positive temperature difference, one is expanding whereas the other layer is contracting causing bending motion.

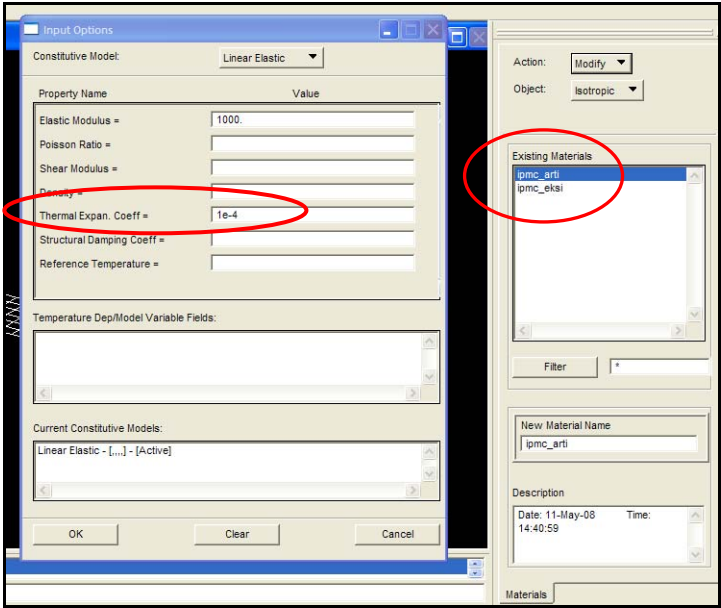


Figure 5.3 Defining the materials of layers

To obtain the bending action, layers are defined by creating laminate composite material. As shown in Figure 5.3, two layers, one with positive thermal expansion coefficient and the other with negative thermal expansion coefficient, are defined sequentially. Thicknesses of the layers were set to half of the thickness of IPMC strip.

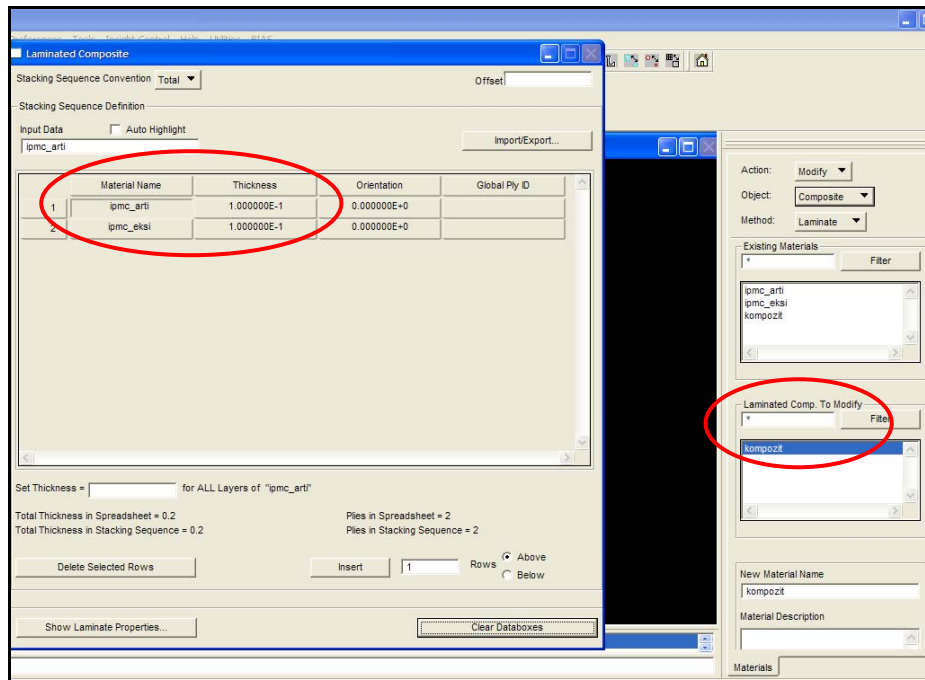


Figure 5.4 Defining composite material

To perform thermo-mechanical coupled analysis, initial temperature and temperature were defined as load and boundary conditions. The reason of defining both initial temperature and temperature separately is that thermal deformation and thermal stress is directly proportional to the change in temperature of the structure.

Initial temperature of the all nodes was taken as zero, and voltage difference was applied to the all nodes as temperature. So that temperature difference is equal to voltage difference.

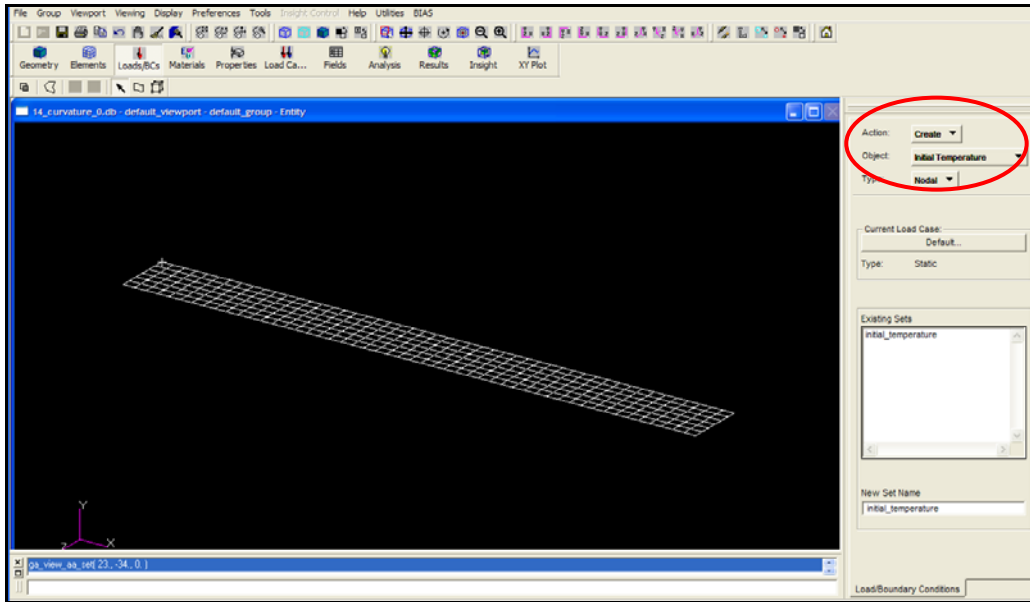


Figure 5.5 Applying initial temperature to IPMC

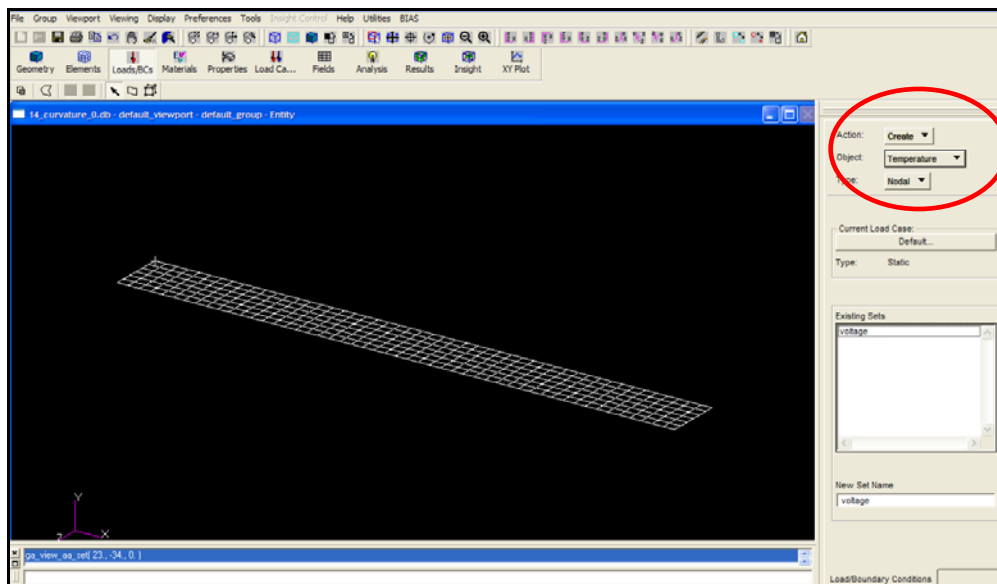


Figure 5.6 Applying temperature to IPMC

Preliminary efforts were to duplicate the results by Lee et al. for IPMC beam of 20 mm in length, 5 mm in width and 300 μm in thickness. The results from our MD.NASTRAN analysis and from Lee et. al matched very well indicating thermal equivalent problem for electromechanical loading was also simulated successfully by our model[86].

CHAPTER 6 RESULTS AND DISCUSSION

6.1. Surface Morphology

In order to characterize the surface morphology of the IPMC, atomic force microscopy (AFM) and scanning electron microscope (SEM) were used. Representative AFM image (surface analysis of IPMC) is presented in Figure 6.1. The surface of IPMC appears to be coated by granular formation of platinum metal with peak/valley depth of approximately 50nm. This granular nano-roughness is responsible for producing a high level of electric resistance, yet provides a porous layer that allows water movement in and out of the membrane.

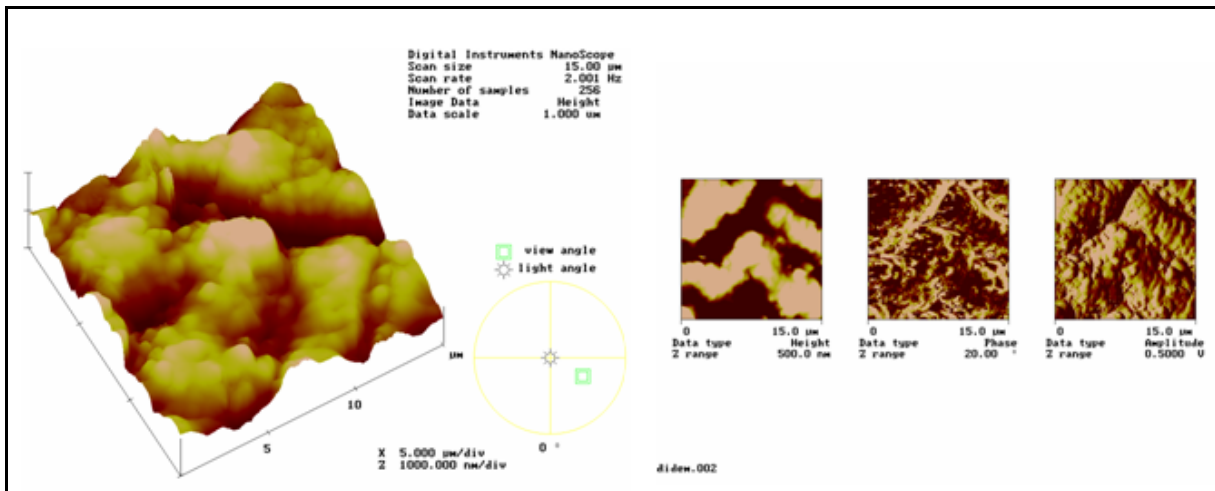


Figure 6.1 AFM results of IPMC actuator surface

During the AFM study, it was also found that platinum particles are dense and, to some extent, possess coagulated shapes. Determination of the size of the deposited platinum particles requires transmission electron microscope (TEM) analysis [113], which was not available for this work.

In addition, scanning electron microscope (SEM) images of the surfaces of coated IPMCs indicate a two-part construction of these materials. Beyond the surface of the membrane, a thicker overlayer of metal is deposited Figure 6.2. IPMC's dendritic structure is formed by platinum particles during plating can be also easily seen in Figure 6.2.

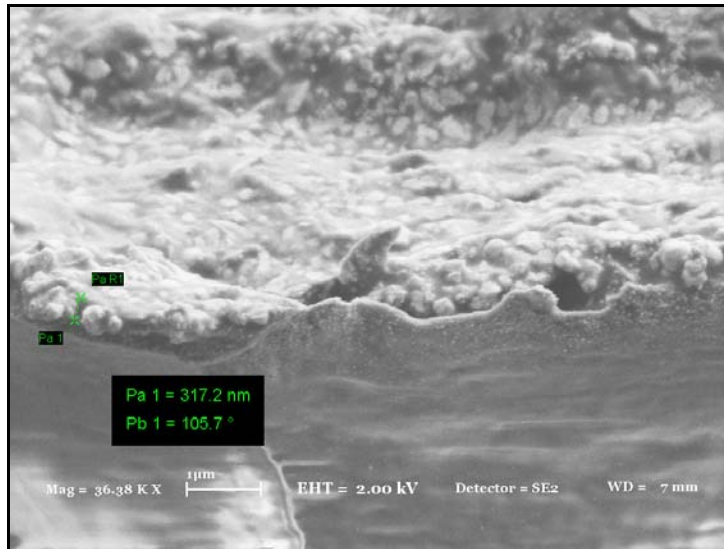


Figure 6.2 SEM analyze of IPMC

The metal electrodes on both sides of an IPMC usually appear with cracks on the surface of IPMC which can be easily seen as in Figure 6.3. Note that Pt electrode and Nafion[®] can be seen through the deep surface crack. These cracks which are formed during fabrication are undesirable because the most important disadvantage of them is breaking the electrode continuity. As a result the performance of IPMC actuators decreases.

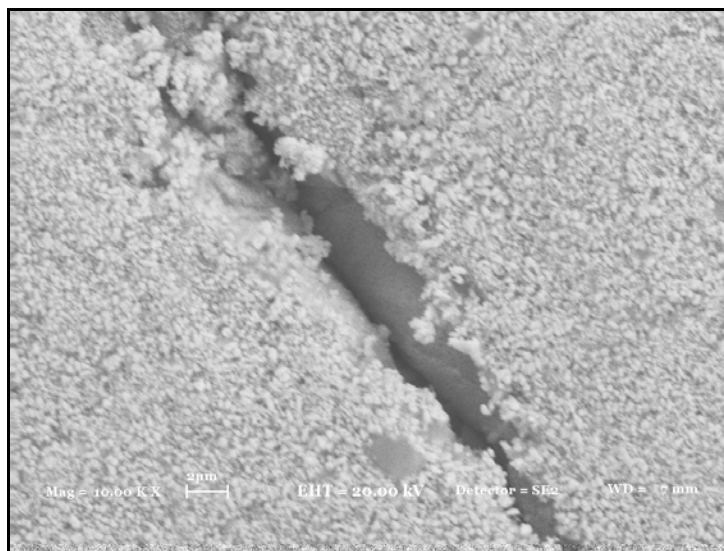


Figure 6.3 Example of surface crack which is detected by SEM

It is presumed that water swelling and electroactive bending generate these fractured structures when the resulting strains exceed the tensile strength of the thin metal layer. This process is not well studied, and anecdotal evidence suggests that IPMC actuators [42, 69].

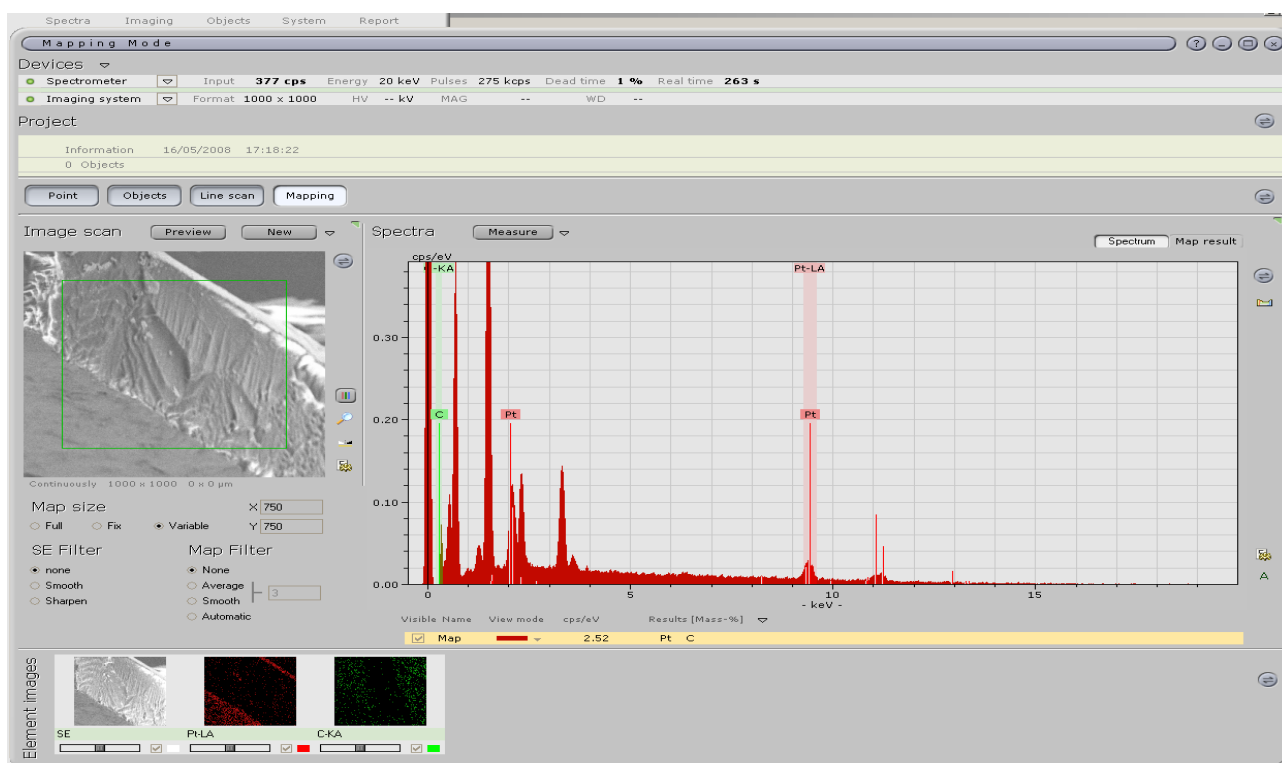


Figure 6.4 EDS measurements through whole structure of IPMC actuator

In order to analyze the elements within the whole structure energy dispersive spectroscopy (EDS) measurements were also carried out. According EDS analysis indicated in Figure 6.4 carbon peaks (green) and platinum peaks (red) were obtained. These aforementioned elements are predominantly found in IPMC. With the help of EDS measurement distribution of Pt along the cross section is noticeable. In Figure 6.5, line scan graph shows that Pt concentration, which is red lines, is increasing along the surface.

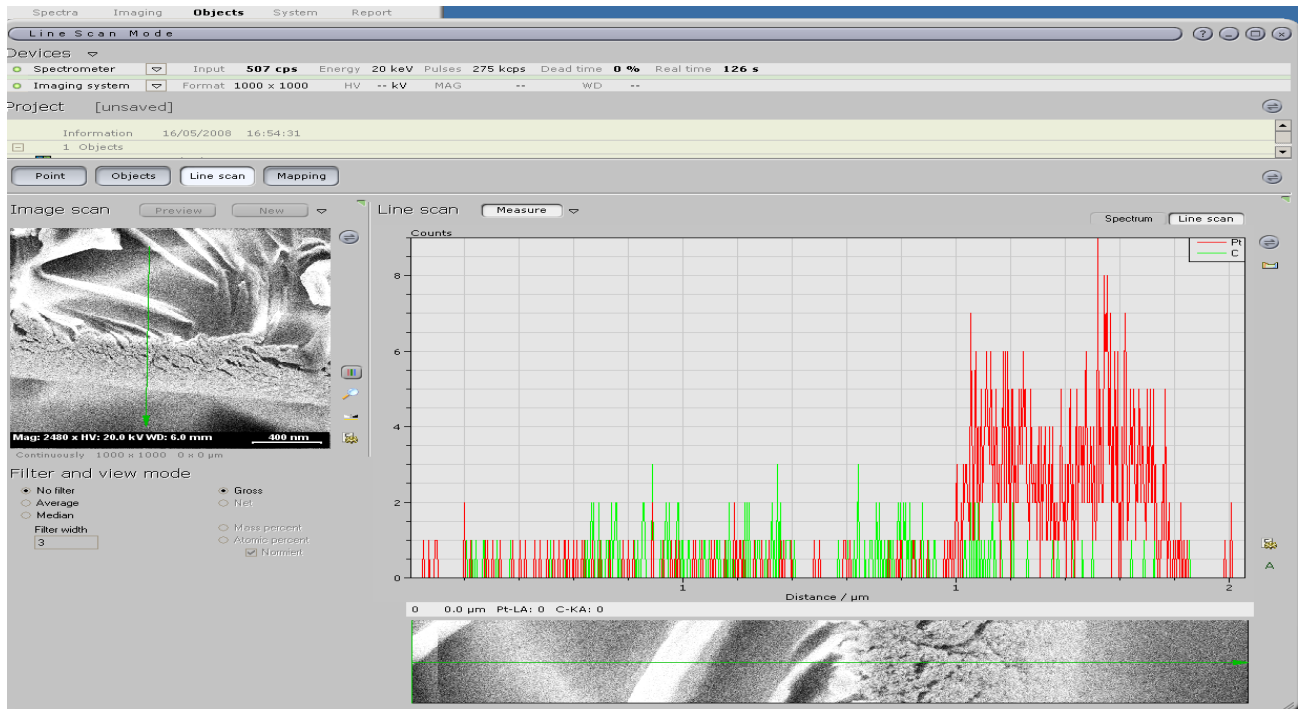


Figure 6.5 EDS measurements of IPMC actuator

6.2. “Equivalent” electromechanical coupling coefficient by unblocked tip displacement study

6.2.1. Effect of IPMC thickness and applied voltage – quasistatic actuation

Firstly in the experimental part of this work, three IPMC actuators were tested following design of experiment summarized in the second and third columns of Table 6.1 where the three replications and their average are also reported. The average data is also shown in Figure 6.6.

Experiments were carried out for each of the three actuators namely 70, 110, and 200 μm thick, flat IPMC actuators at quasi-static excitation voltage of 0.5, 1.0, 1.5 and 2.0 V. The combinations of the thickness and voltage resulted 12 test points as indicated in Table 6.1. At each test point, excitation and measurement of resultant tip displacement were repeated 3 times. Averages of the three measurements at each test point were then considered as the result of the associated combination of thickness and applied voltage.

Table 6.1 Measured free tip displacements according to various thickness and voltage values

Test no	Thickness H (μm)	Applied voltage, V (Volt)	Free Tip Displacement, s (mm)				Surrogate \hat{S}_{av} (mm)	%Error (\hat{S}_{av} vs S_{av})
			Test 1, s_1	Test 2, s_2	Test 3, s_3	Average, s_{av}		
1	70	0.5	0.834	0.834	0.500	0.723	0.666	7.83
2	70	1	1.501	1.667	1.333	1.500	1.551	3.38
3	70	1.5	1.834	2.750	1.667	2.084	2.152	3.28
4	70	2	2.501	3.334	2.500	2.778	2.716	2.25
5	110	0.5	0.834	2.501	0.834	1.390	1.4863	6.97
6	110	1	1.667	3.334	1.667	2.223	2.104	5.33
7	110	1.5	2.501	4.168	2.201	2.957	2.903	1.81
8	110	2	3.334	5.001	3.830	4.055	4.130	1.85
9	200	0.5	3.334	2.084	2.167	2.528	2.488	1.59
10	200	1	3.334	5.001	5.830	4.722	4.789	1.44
11	200	1.5	10.002	6.668	8.330	8.333	8.318	0.18
12	200	2	13.336	13.336	13.330	13.334	13.321	0.09

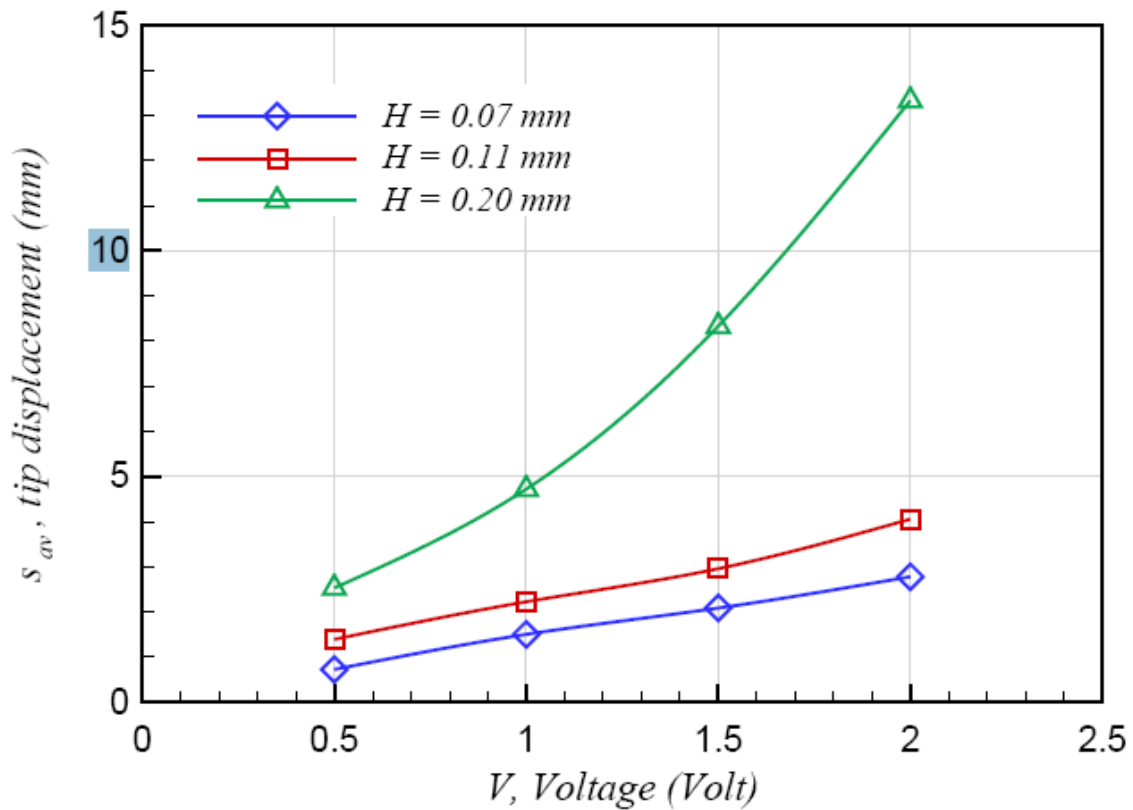


Figure 6.6 Unblocked Tip displacement – voltage relationship for various thicknesses

The actuation behavior of IPMC strips depends on two specific parameters; magnitude and frequency of the applied electric field. As magnitude of the electric field increases, displacement of IPMC strip increases. As can clearly be seen from the Figure 6.6 above experimentally observed data verify that actuation increases with the applied electric field.

With these observations cases show that our specimens are working properly and appropriate for finite element and optimization analysis.

By using average displacement values used in statistical analysis software, JMP version 5.1. Average displacement equation approximated by least square regression. Then Equation 6.1 was obtained as the polynomial fit predicting the tip displacement as a function of voltage and thickness of IPMC strip.

$$\begin{aligned} \hat{s}_{av} = & -5.524 + 86.927H + 9.908V - 267.343H^2 \\ & -118.511HV - 3.182V^2 + 390.475H^2V + 23.25HV^2 + 0.329V^3 \end{aligned} \quad (6.1)$$

Using thickness and voltage data in the obtained semi-empirical effective coupling constant equation, predictions of displacement obtained via surrogate function.

The fitting statistics are quite good: $R^2 = 0.999$, root mean square error (RMSE) of 0.133 with the mean of response based on the 12 points 3.885, corresponding to a coefficient of variation (RMSE/Mean of the data) of about %3. The second column of Table 6.1 from the right end summarizes the prediction of the tip displacements by Eq. 6.1 and the last column is the relative percent error when compared to the experiment average measurements. And by comparing experimental and predicted average displacement values maximum difference about 8% as shown in the table only for 12 data.

The effective electro-mechanical coupling coefficient, d_{31} , can now also be predicted by substituting Eq. 6.1 into Eq. 5.4 which is substitute \hat{s}_{av} as the tip displacement s , resulting Eq.6.2 which is an approximation for the coefficient, \hat{d}_{31} when the beam is straight or flat:

$$\hat{d}_{31} = \frac{2H^2}{3VL^2} \hat{s}_{av} \quad (6.2)$$

The “effective electro-mechanical coupling coefficient” can be calculated from Eq. 6.2 by using the tip displacement values obtained from clamped-free IPMC actuator tests. This

effective coefficient is an essential component in this study as it enables the use of commercial finite element software in simulating the IPMC behavior when excited.

The comparison of coupling coefficient by Eq. 6.2 (using the average measured tip displacements) and Eq. 5.4 is given in Table 6.2. The relative errors are the same as in tip displacements, because the only difference is the use of measured s as opposed to approximated tip displacement \hat{s}_{av} .

Table 6.2 Comparison of electro-mechanical coupling coefficients obtained by Eq. 5.4 (with s_{av}) and Eq. 6.2 (with \hat{s}_{av})

Applied Voltage	H=70 μm		H= 110 μm		H= 200 μm	
	d_{31} test average [$\mu\text{m}/\text{V}$]	\hat{d}_{31} [$\mu\text{m}/\text{V}$]	d_{31} test average [$\mu\text{m}/\text{V}$]	\hat{d}_{31} [$\mu\text{m}/\text{V}$]	d_{31} test average [$\mu\text{m}/\text{V}$]	\hat{d}_{31} [$\mu\text{m}/\text{V}$]
0.5	1.889E-03	1.741E-03	8.96E-03	9.591E-03	5.394E-02	5.308E-02
1	1.960E-03	2.027E-03	7.172E-03	6.789E-03	5.036E-02	5.109E-02
1.5	1.815E-03	1.874E-03	6.360E-03	6.245E-03	5.926E-02	5.915E-02
2	1.815E-03	1.774E-03	6.542E-03	6.663E-03	7.111E-02	7.105E-02

The tip displacement and coupling coefficient variation within the parameter space of voltage and thickness bounded in 0.5-2 Volts and 70-200 micron respectively is presented in Figure 6.8 as contour plots. It can be concluded that the coefficient is greatly affected by the thickness of the IPMC. The effect of applied voltage is not significant if the thickness is small, but gets more pronounced as the thickness increases.

6.2.2. Finite element simulations of straight IPMC actuators

Based on the test results in Table 6.2, the “equivalent” or “effective” electro-mechanical coupling coefficients, d_{31} , and equivalent thermal expansion coefficients α for NASTRAN linear static analysis were calculated by using Eq. 5.3 and Eq. 5.4, respectively. The results of finite element analyses by MD.NASTRAN and the test results perfectly matched as it should be.

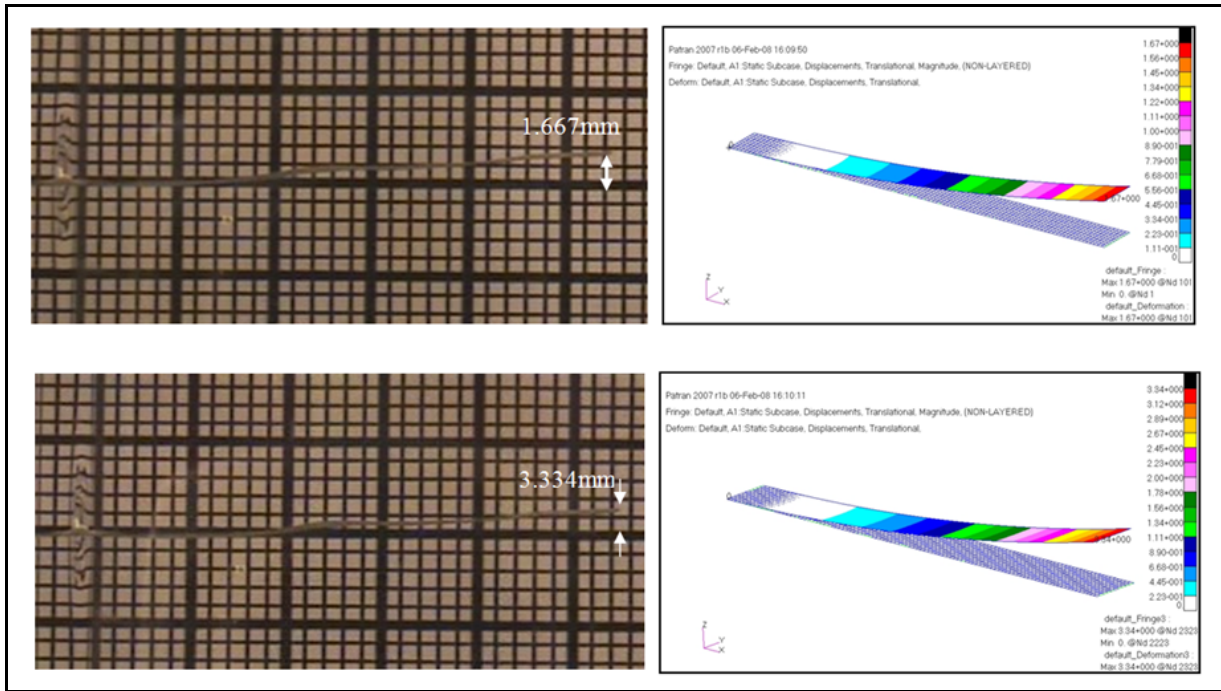


Figure 6.7 Finite element analyses and experimental results for thickness of 70 μm thick IPMC test specimen at applied voltage 1 V 70 μm at 1 and 2 Volts, resulting in 1.667 mm and 3.334 mm, respectively (Test 2 column of Table 6.1).

In Figure 6.7, for instance comparison of experimental and simulation results can be seen for the test specimen having thickness of 70 μm thick IPMC test specimen at applied voltage 1V and 2V (test 2 column of Table 6.1).

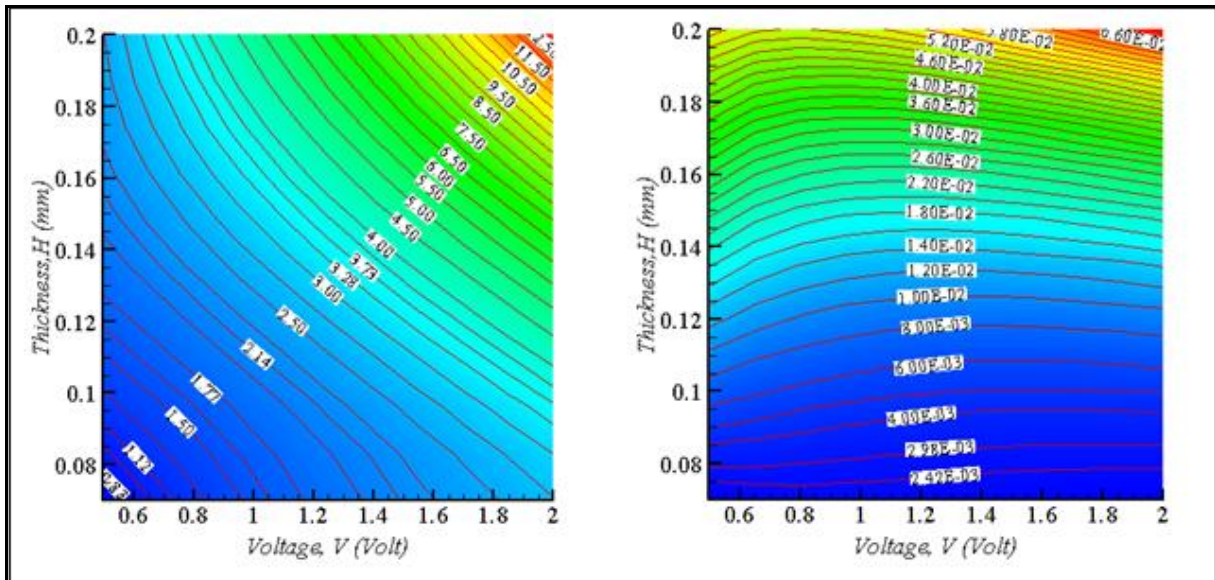


Figure 6.8 Prediction contours, tip displacement, ξ_{av} (Left) and equivalent coupling coefficient, d_{31} (right).

The tip displacement and coupling coefficient variation within the parameter space of voltage and thickness bounded in 0.5-2 Volts and 70-200 micron respectively is presented in Figure 6.8 as contour plots. It can be concluded that the coefficient is greatly affected by the thickness of the IPMC. The effect of applied voltage is not significant if the thickness is small, but gets more pronounced as the thickness increases.

The tip displacement measurement was $s_{measured} = 1.667$ mm and associated coefficient due to Eq. 5.4 is $d_{31} = 2.178 \times 10^{-3} \mu\text{m}/\text{V}$. Using this equivalent coupling coefficient, the deflected shape of the IPMC by the MD.NASTRAN was obtained as shown in Figure 6.7, where the tip displacement $s = 1.67$ mm. Similar comparison was also presented for the IPMC strip with thickness of 200 μm tested at 1 V (test 1 column of Table 6.1). The tip displacement was $s_{measured} = 3.334$ mm and associated coefficient was found to be $d_{31} = 3.556 \times 10^{-2} \mu\text{m}/\text{V}$. The results of the finite element analyses by MD.NASTRAN and the test results perfectly match as it should be, because the “equivalent” coefficient used in the “straight” IPMC beam numerical (FE) analysis is derived from the analytical/exact solution of the “straight” equivalent beam.

6.2.3. Finite element simulations of curved IPMC actuators - Effect of initial curvature

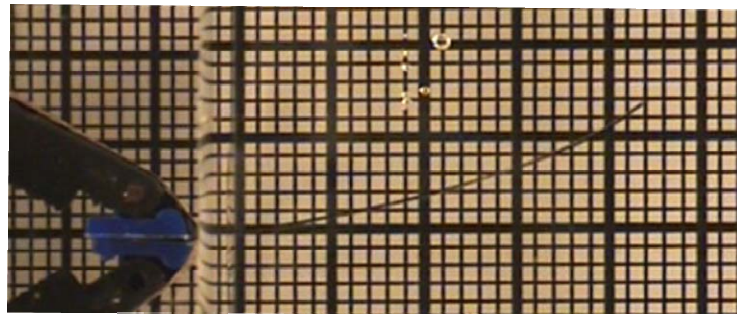


Figure 6.9 The curved IPMC strip used in the experiments

For initially straight IPMC specimens, as the equations for equivalent bimorph beam model are derived for a straight beam, the displacements measured in the tests and finite element results are perfectly consistent. However, when handling and immersing IPMC into water or deliberately, an initial curvature may be imposed even before voltage is applied. Figure 6.9 shows an example for such a case. Radius of curvature ρ can be approximately determined using the tip displacement, s

$$\rho = \frac{1}{\kappa} \cong \frac{L^2 + s^2}{2s} \quad (6.3)$$

where κ and L are the curvature and length of the strip, respectively [114]. For the case of initial curvature, s_0 is the initial tip displacement prior to actuation. The IPMC strip in Figure 6.9, for instance has initial tip displacement $s_0 \sim 8$ mm which corresponds to preset radius of curvature $\rho_0=157$ mm.

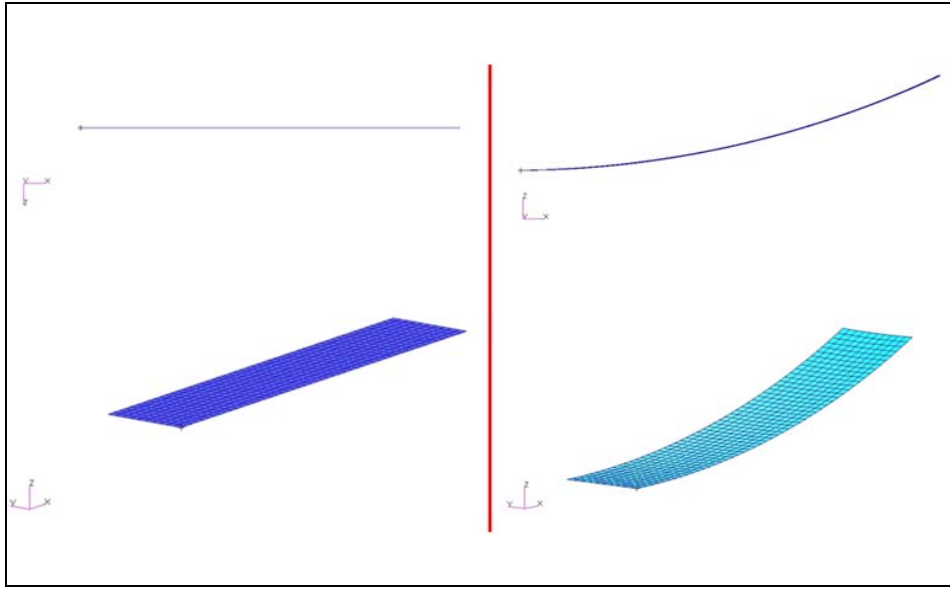


Figure 6.10 Finite element models of beams

In order to evaluate the effect of the initial or preset curvature, test results and the finite element analyses for the initially curved IPMC actuator were compared while the coupling coefficient is still obtained from equivalent “straight” bimorph model of Figure 5.1 and Eq. (5.4). Measurement at 1V on the test specimen (50 mm x 5 mm x 0.2 mm) with preset curvature ($\rho_0 = 157$ mm, Figure 6.39) was performed. The resultant tip displacement relative to the initial tip position of the curved beam was measured as $s_{measured} = 4.00$ mm. Then, the “equivalent” electro-mechanical coupling coefficient was computed by the Eq. (5.4) substituting $s_{measured}$, and found as $(d_{31})_{straight} = 4.267 \times 10^{-2} \mu\text{m/V}$. Using $(d_{31})_{straight}$ the initially curved beam MD.NASTRAN analysis resulted in tip displacement $s_{curved} = 3.89$. The difference between s_{curved} and $s_{measured}$ is due to the fact that coefficient used in the curved beam analysis is from Eq. (5.4) of the “straight” beam model. When we use the straight beam

NASTRAN model, 4.01 mm displacement was obtained, but the computed deformed shape does not match with the experimentally observed shape as shown in figure 6.11.

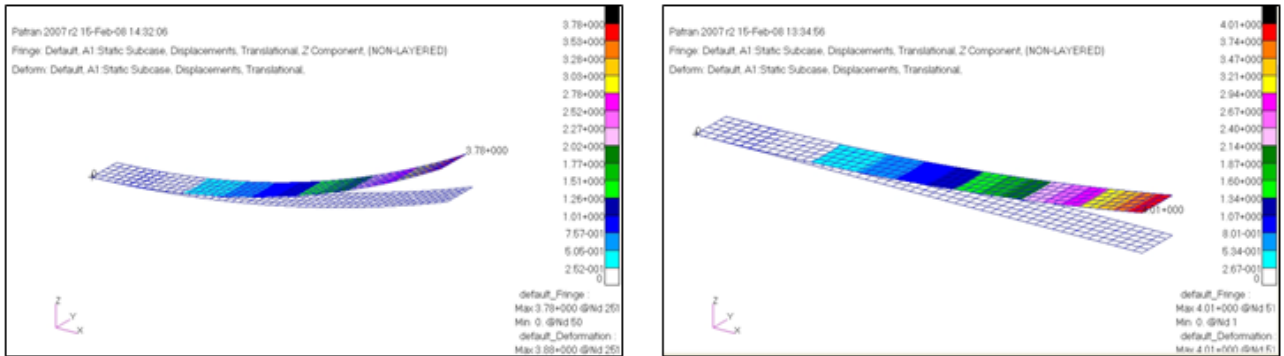


Figure 6.11 Finite element results for curved (left) and straight beam (right)

In order to predict the tip displacement and the deformed shape accurately, the “equivalent” coupling coefficient needs also to take into account the preset curvature when the specimen or the beam is not initially straight. A simplest way to include the preset curvature effect is to find whether a tuning or correction factor can be introduced to the coupling coefficient expression,

$$(d_{31})_{\kappa} = c_{\kappa} \frac{2H^2}{3VL^2} s \quad (6.4)$$

where c_{κ} is the correction factor for initial curvature. Comparing the MD.NASTRAN results for the curved and straight beams, Figure 6.11, with the effective coefficient by Eq. (5.4), the tip displacements of the curved and straight beams of relate as,

$$s_{curved} = 0.97 * s_{straight} \quad (6.5)$$

where $s_{straight} = s_{measured}$ (due to original equivalent “straight” bimorph beam model). That is, to tune the tip displacement by the curved model, the effective coupling coefficient should be corrected by a factor of $c_{\kappa}=1.03$ determined by the following,

$$c_{\kappa} = \frac{s_{straight}}{s_{curved}} \quad (6.6)$$

The next immediate question is whether this correction factor is also dependent to the thickness of the membrane. Similar calculations were performed for the 70 and 110 μm thick

IPMC actuators. The comparison between the straight and curved models resulted in the same correction factor provided that the pre-imposed curvature is fixed. That is, the membrane thickness does not affect the correction factor due to initial curvature.

The magnitude of the correction factor, on the other hand, is for a specified curvature which is expected to change for different initial curvature, and c_k may be expressed as function of the initial radius of curvature, ρ_0 . In addition to $\rho_0 = 157$ mm already studied, several other ρ_0 values were considered as indicated in Table 6.3.

Table 6.3 Initial curvature effect and correction on equivalent coefficient, the tip displacement of the straight beam analysis $s_{straight} = 4$ mm, and associated coefficient $d_{31} = 4.267 \times 10^{-2} \mu\text{m/V}$ due to Eq. (5.4) when 1V is applied

s_0 initial tip disp. [mm]	ρ_0 initial radius of curvature, [mm]	s_{curved} tip disp. [mm]	c_k Correction factor	$(d_{31})_k$ [$\mu\text{m/V}$]
1.0	1251	4.001	1.002	4.268×10^{-2}
2.0	626	4.000	1.002	4.269×10^{-2}
3.0	417	3.980	1.007	4.290×10^{-2}
4.0	313	3.971	1.009	4.300×10^{-2}
5.0	251	3.955	1.013	4.317×10^{-2}
6.0	209	3.925	1.021	4.350×10^{-2}
8.0	157	3.900	1.028	4.378×10^{-2}
10.0	126	3.867	1.036	4.415×10^{-2}
12.5	101	3.780	1.060	4.516×10^{-2}
15.0	84	3.672	1.092	4.650×10^{-2}

It is sufficient to compare the tip displacements from NASTRAN analyses of the initially curved strips with the tip displacement of the straight strip analysis. The later is the analysis mentioned earlier, resulting $s_{straight} = 4.01$ mm and $(d_{31})_{straight} = 4.267 \times 10^{-2} \mu\text{m/V}$. The analyses by MD.NASTRAN for the initially curved beams where $(d_{31})_{straight}$ was implemented in the models and the resultant tip displacements s_{curved} for 1V were obtained as reported Table 6.3.

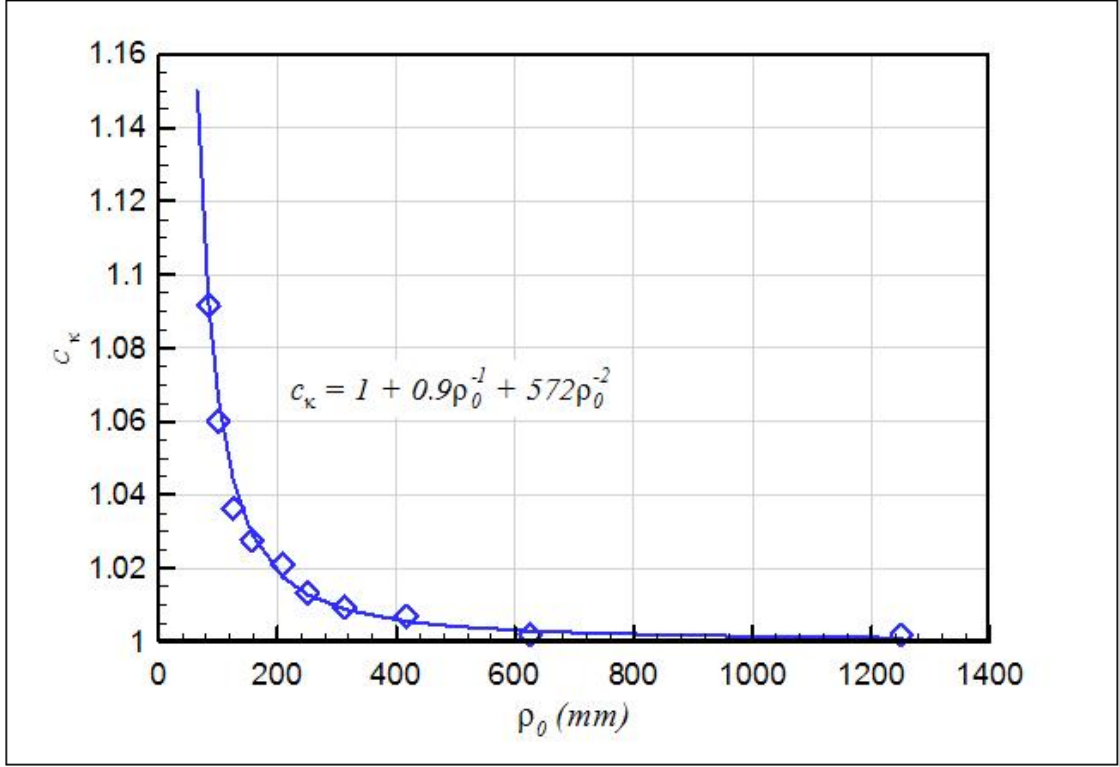


Figure 6.12 Variation of the correction factor versus initial radius of curvature

The correction factors on the coupling coefficient associated with the radii of curvature were then obtained by Eq. (6.6). Figure 6.12 shows how correction factor varies versus initial radius of curvature where the data is also fit by the Eq. (6.7),

$$\hat{c}_k = 1.0 + 0.9\rho_0^{-1} + 572\rho_0^{-2} \quad (6.7)$$

The approximation for “effective” electromechanical coupling coefficient can now be updated in order to take into account the initial or pre-imposed curvature if any. That is Eq. (6.2) can be corrected by the Eq. (6.7),

$$\hat{d}_{31} = \hat{c}_k \frac{2H^2}{3VL^2} \bar{s}_{av}$$

$$\hat{d}_{31} = \frac{2H^2}{3VL^2} \left[\begin{array}{l} -5.524 + 86.927H + 9.908V - 267.343H^2 \\ -118.511HV - 3.182V^2 + 390.475H^2V + 23.25HV^2 + 0.329V^3 \end{array} \right] \left(1.0 + 0.9\rho_0^{-1} + 572\rho_0^{-2} \right) \quad (6.8)$$

To sum up, in order to use the equivalent bimorph model by using test outputs for the required material properties for finite element analysis, necessary updates should be done if a curved beam is used.

6.2.4. Effect of frequency

As mentioned before actuation affected by magnitude and frequency of applied electric field. In this part the effect of frequency of the applied electric field is discussed, actuation-frequency relationship analyzed and observed data is presented below;

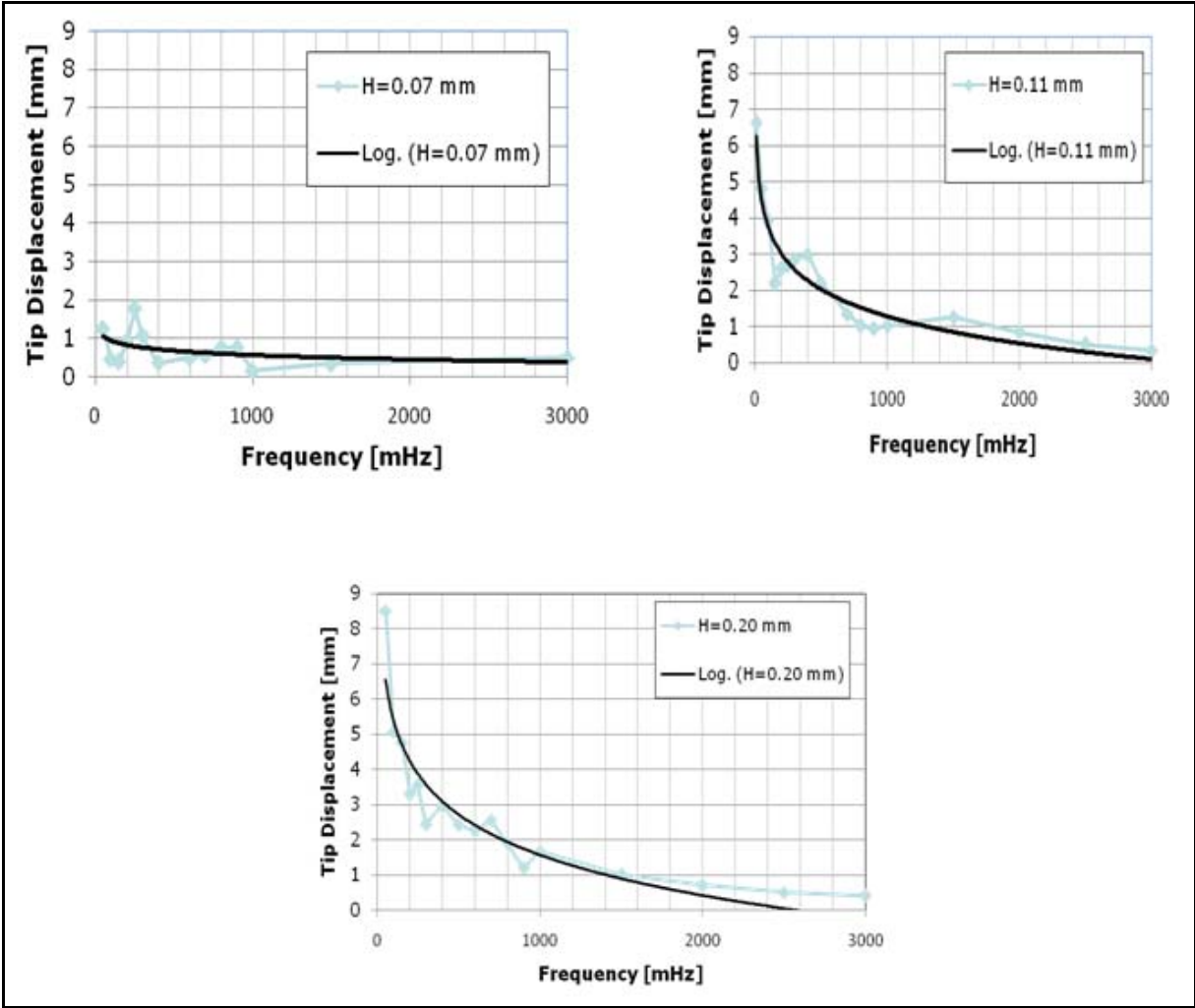


Figure 6.13 Frequency vs. tip displacement graphs

Actuation-frequency trend data of IPMC strips, having thicknesses of 70,110 and 200 μ m, in the frequency range from 0.01 Hz to 3 Hz are shown in the figures above. As shown in figures the increase in frequency causes the tip actuation to decrease. That is the free tip displacement is a decaying function of the excitation frequency.

6.3. “Equivalent” young’s modulus by unblocking force study

The equivalent bimorph beam model also features “equivalent” young’s modulus E as “equivalent” physical properties of IPMCs: along with the electro-mechanical coupling coefficient, d_{31} . The experimental output necessary to calculate this property is the blocking force at the tip of the actuator that is the force that the tip of the actuator applies when the displacement is blocked. According to the equivalent bimorph beam model, effective coupling coefficient d_{31} and young’s modulus can be written as:

$$E = \frac{8LF_{bl}}{3WHd_{31}V} \quad (6.9)$$

where F_{bl} is the blocking force. As demonstrated in the equations (5.3) and (6.9), free tip displacement and blocking force are compulsory to find the equivalent physical properties of IPMCs.

Maximum that is free tip displacement was first measured after the specified voltage was applied to the IPMC strip. To calculate the equivalent young’s modulus of IPMC strip, blocking force should also be measured. We measured the blocking force values for the specimen having thickness $200\mu\text{m}$ with force transducer at 2 Volt at a minimal frequency, 10mHz.

The experimental results and “equivalent” elastic modulus by using Eq. (6.9) is reported in Table 6.4.

Table 6.4 Geometric and Characteristic values of IPMC actuator

H [mm]=	0.20
L [mm]=	50.00
W [mm]=	5.00
V[V]=	2.00
s [mm]=	15.23
d_{31}[mm/V]=	$8.1227E^{-05}$
F_{Exp} [N]=	0.00147
E_{Exp} [MPa]=	1206

Note that in paper of Lee et. al. the equivalent young’s moduli for 2V is 1133 MPa.[88]

6.3.1. Finite element simulations of straight IPMC actuators for force measurement

In order to verify the “equivalent” properties of IPMC they were implemented together in Finite Element Analyses. The aim was to see, given the “equivalent” electro-mechanical coupling coefficient at a specified electric field excitation, whether the IPMC actuator would apply a contact force at the tip as a result of its “equivalent” mechanical property, E, when the movement is constrained by the contact. The analysis was performed in MD.Nastran and tip displacement was found 15.2mm as shown in Figure 6.14. This indicates that tip displacement obtained from experiment, which is 15.23mm as in Table 6.4, and analysis results show good correlation.

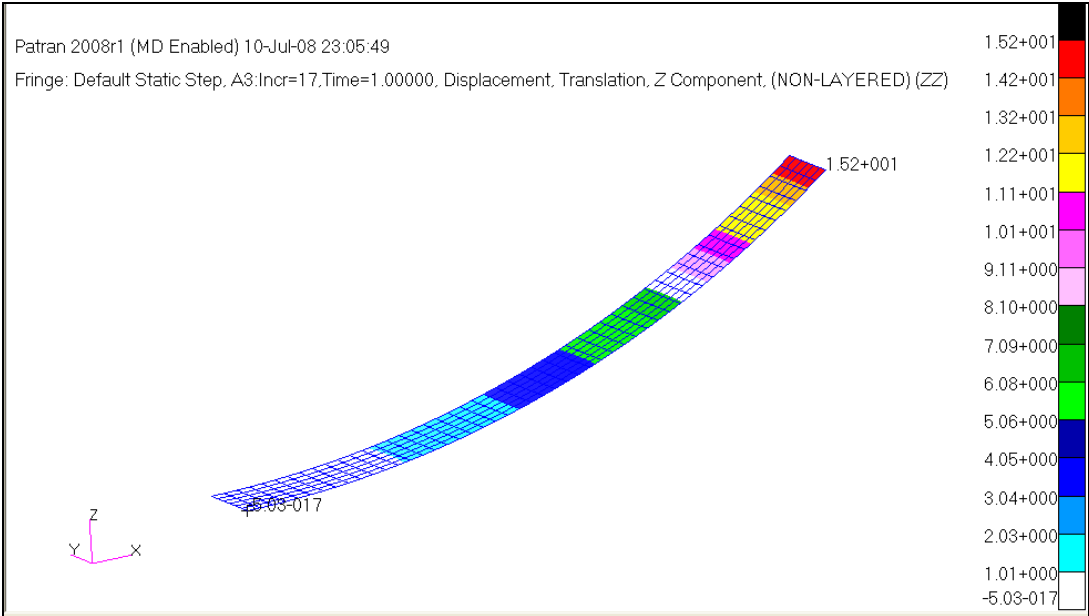


Figure 6.14 Finite Element result

In the experiments, load cell position was adjusted to obtain an initial condition which is the contact of the IPMC actuator tip to the surface of load cell. After this condition was established, electrical load is applied and force was monitored. To find the blocking force using MD.Nastran, a rigid surface was created to simulate the load cell surface as shown in Figure 6.15 between the rigid surface and nodes at the edge of IPMC contact was defined. This is the new feature of MD.Nastran and it is called as linear contact. This contact algorithm accounts for the shell thickness so to simulate the experiment, rigid surface created half of the thickness above the IPMC strip’s neutral plane.

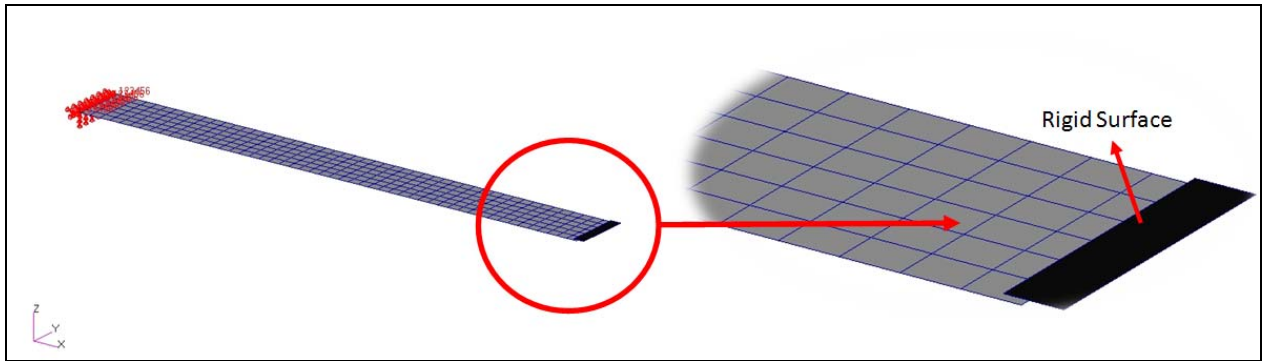


Figure 6.15 Modelling of rigid surface and contact

During post-processing, firstly, tip displacement and behaviour of the IPMC strip was controlled in order to be sure that no penetration occurred during simulation. After checked that contact between the two bodies works fine, the force acting on the rigid surface was plotted.

On the other hand experimentally observed force value is 0.00147N. The result obtained by using FEA is 0.001297 and the difference between the measured and calculated forces is about 12%, which is reasonable considering the imperfections that are not modeled in the FEA, such as the strip being not ideally straight (Figure 6.9).

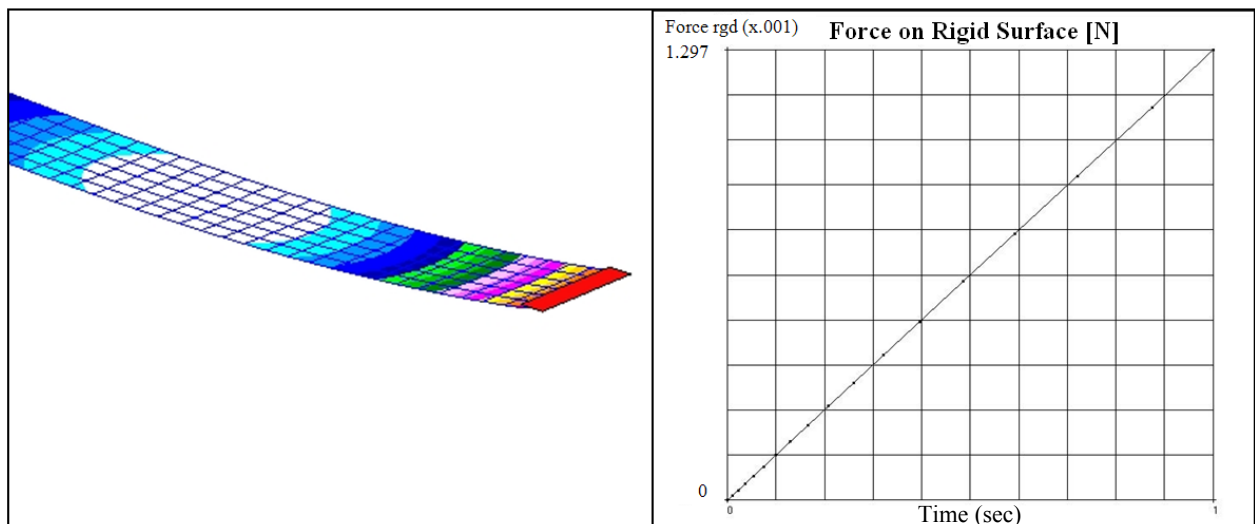


Figure 6.16 Force acting to the rigid surface

CHAPTER 7 CONCLUSION

7.1 Concluding remarks

An investigation on the fabrication of IPMC actuator strips from commercial Nafion[®] ion exchange membranes in various thicknesses was performed. The implementation of “equivalent” bimorph beam model was carried out and two “equivalent” material properties, “equivalent” electro-mechanical coefficient and “equivalent” young’s modulus were determined. The thesis showed first results on how the IPMC thickness, applied voltage and preset curvature affect the equivalent electro-mechanical coupling coefficient in equivalent bimorph beam approach. Three different thickness and and four excitation voltages, were studied and experiments and finite element analyses using MD.NASTRAN were performed at all twelve combinations for the two main factors. Particularly, a semi-empirical approximation of the equivalent electro-mechanical coupling coefficient was proposed for the IPMC thickness and voltage ranges investigated in this study. In addition, “equivalent” young’s modulus was determined by combining the blocking force measurements and the “equivalent” bimorph beam model. Based on the results following remarks can be made:

- Electro-mechanical coupling coefficient due to equivalent bimorph model was treated to be an “equivalent” or “effective” parameter, not an actual material constant as it changes with the IPMC thickness and applied voltage.
- For preliminary design purposes, an approximation of the equivalent coefficient with good accuracy was obtained for straight IPMC actuators.
- Initial or preset curvature of the strips before electrical excitation also influenced the “equivalent” coupling coefficient and its effect was included by a correction factor approach.
- The corrected approximation for the “equivalent” coupling coefficient enables to incorporate the thickness and preset curvature of the IPMC as design parameters.
- The “equivalent” properties, electromechanical coefficient and young’s modulus by the equivalent bimorph beam model works reasonably well in calculating the actuation force at the tip by MD. NASTRAN.
- These “equivalent” material properties can be easily implemented in preliminary design of actuator made of IPMC.

REFERENCES

- [1] Smart Structures and Materials Book, Brian Culshaw, Artech House INC., 1996, Chapter1
- [2] Smart Material, http://en.wikipedia.org/wiki/Talk:Smart_material, last accessed on 15.07.07.
- [3] http://www.cs.ualberta.ca/~database/MEMS/sma_mems/smrt.html, last accessed on 15.07.07.
- [4] http://www.electronics.ca/reports/materials_polymers/actuators.html, last accessed on 18.07.07.
- [5] Yoseph Bar-Cohen, Artificial Muscles using Electroactive Polymers (EAP): Capabilities, Challenges and Potential. Artificial Muscles using Electroactive Polymers (EAP)
- [6] Yoseph Bar-Cohen, Transition of EAP material from novelty to practical applications— are we there yet?, Proceedings of EAPAD, SPIE's 8th Annual International Symposium on Smart Structures and Materials, 5-8 March, 2001, Newport, CA. Paper No. 4329-02.
- [7] <http://electrochem.cwru.edu/ed/encycl/art-p02-elact-pol.html>, last accessed on 18.07.08.
- [8] Shahinpoor, M., Kim, K.J., “Ionic polymer–metal composites: I. Fundamentals,” Smart Mater. Struct. (10), 819–833 (2001).
- [9] <http://trs-new.jpl.nasa.gov/dspace/bitstream/2014/37531/1/05-0308.pdf>, last accessed on 10.07.07.
- [10] Jaehwan Kim, Chun-Seok Song, Sung-Ryul Yun, ‘Cellulose based electro-active papers: performance and environmental effects’ Smart Mater. Struct. 15 719-723 (2006)
- [11] <http://ndea.jpl.nasa.gov>, last accessed on 18.07.07
- [12] Feynman, R. P., Surely You’re Joking, Mr. Feynman!, First Ed., New York:W.W. Norton, 1985.
- [13] Bergman, I. (Minister of Power, London), “Improvements in or relating to membrane electrodes and cells,” GB Patent: 1,200,595, 1970.
- [14] McCallum, C., and Pletcher, D., “Reduction of oxygen at a metallized membrane electrode,” Electrochim. Acta, v. 20, no. 11, 1975, pp. 811-814.
- [15] Levine, C. A., and Prevost, A. L. (Dow Chemical Co.), “Metal plating permselective membranes,” FR Patent: 1,536,414, 1968.

- [16] Hitachi, "Formation of an electrode film on an ion-exchanging membrane" (Hitachi Shipbuilding and Engineering Co., Ltd., Japan), JP Patent: 58,185,790, 1983.
- [17] Sakai, T., Takenaka, H., and Torikai, E. (Agency of Industrial Sciences and Technology, Japan), "Metal-containing ion-exchange membranes for gas separation," JP Patent: 60,135,434, 1985a.
- [18] Sakai, T., Takenaka, H., Wakabayashi, N., Kawami, Y., and Torikai, E. "Preparation of Nafion-metal fine particle composite membranes," Osaka Kogyo Gijutsu Shikensho Kiho, v. 36, no. 1, 1985b, pp. 10-16.
- [19] Millet, P., Pineri, M., and Durand, R., "New solid polymer electrolyte composites for water electrolysis," J. Appl. Electrochem., v. 19, no. 2, 1989, pp. 162-166.
- [20] Millet, P., Durand, R., and Pineri, M., "Preparation of new solid polymer electrolyte composites for water electrolysis," Int. J. Hydrogen Energy, v. 15, no. 4, 1990, pp. 245-253.
- [21] Millet, P., Durand, R., Dartyge, E., Tourillon, G., and Fontaine, A., "Study of the precipitation of metallic platinum into ionomer membranes by time-resolved dispersive x-ray spectroscopy," AIP Conf. Proc., 1992, v. 258, pp. 531-538.
- [22] Millet, P., Durand, R., Dartyge, E., Tourillon, G., and Fontaine, A., "Precipitation of metallic platinum into Nafion ionomer membranes. I. Experimental results," J. Electrochem. Soc., v. 140, no. 5, 1993, pp. 1373-1380.
- [23] Millet, P., Andolfatto, F., and Durand, R., "Preparation of solid polymer electrolyte composites: investigation of the ion exchange process," J. Appl. Electrochem., v. 25, no. 3, 1995, pp. 227-232
- [24] Kordesch, K. v., and Simader, G. R., "Environmental impact of fuel cell technology," Chem. Rev., v. 95, no. 1, 1995, pp. 191-207.
- [25] Sadeghipour, K., Salomon, R., and Neogi, S., "Development of a novel electrochemically active membrane and 'smart' material based vibration sensor/damper," Smart Mater. Struct, v. 1, no. 2, 1992, p. 172-179.
- [26] Oguro, K., Kawami, Y., and Takenaka, H., "An actuator element of polyelectrolyte gel membrane-electrode composite," Osaka Kogyo Gijutsu Shikensho Kiho, 43, no. 1, 1992, pp. 21-24.
- [27] Mojarrad, M., and Shahinpoor, M., "Ion exchange membrane-platinum composites as electrically controllable artificial muscles," Third International Conference on Intelligent Materials, SPIE Proc. Vol. 2779, 1996, pp. 1012-1017.

- [28] Nemat-Nasser, S., "Micromechanics of Actuation of Ionic Polymer-metal Composites," *J. Appl. Phys.*, v. 92, no. 5, 2002, pp. 2899-2915.
- [29] Nemat-Nasser, S., and Wu, Y., "Comparative Experimental Study of Nafion-and-Flemion-Based Ionic Polymer-metal Composites (IPMC)," *J. Appl. Phys.*, v. 93, no. 9, 2003a, pp. 5255-5267.
- [30] Nemat-Nasser S., and Zamani, S., "Experimental Study of Nafion-and Flemion-Based Ionic Polymer-Metal Composites (IPMC's) with Ethylene Glycol as Solvent," *Proceedings of SPIE*, 5051, 2003, pp. 233-244.
- [31] Nemat-Nasser S. and Chris W. Thomas University of California, San Diego ; Chapter 6 Ionomeric Polymer-Metal Composites, 2001.
- [32] <http://www.asahi-kasei.co.jp/membrane/english/tradenm/t06.html>, last accessed on 28.05.07.
- [33] http://www.agc.co.jp/english/csr/environment/products/positive_seihin5.html, last accessed on 28.05.07.
- [34] <http://en.wikipedia.org/wiki/Nafion>, last accessed on 20.07.07.
- [35] Walther Grot, Fluorinated Ionomers, pg 240 2008 .
- [36] Church Steven (January 6, 2006). "Del. firm installs fuel cell", *The News Journal*, p. B7.
- [37] Heitner-Wirguin, C. "Recent advances in perfluorinated ionomer membranes: structure, properties and applications". *Journal of Membrane Science* 120: 1–33. (1996).
- [38] Mauritz, K. A., Moore, R. B. (2004). "State of Understanding of Nafion". *Chemical Reviews* 104: 4535–4585. (2004).
- [39] <http://www.permapure.com/TechNotes/Nafion%20physical%20&%20chemical.html>, last accessed on 12.07.07.
- [40] Shahram Zamani and Sia Nemat-Nasser, Controlled actuation of Nafion-based Ionic Polymer-metalComposites (IPMCs) with Ethylene Glycol as Solvent, *Smart Structures and Materials 2004: Electroactive Polymer Actuators and Devices (EAPAD)*, edited by Yoseph Bar-Cohen, proceedings of SPIE Vol. 5385 (SPIE, Bellingham, WA, 2004)
- [41] Shahinpoor M., Kim K.J., "Ionic polymer–metal composites: Manufacturing techniques," *Smart Mater. Struct.* 12 65–79 (2003)
- [42] Bar-Cohen Y., Leary S., Yavrouian A., Oguro K., Tadokoro S., Harrison J., Smith J. and Su J., Challenges to the application of IPMC as actuators of planetary mechanisms, *Proceedings of SPIE's 7 Annual International Symposium on Smart Structures and Materials*, 1-5 March, 2000, Newport, CA. Paper No. 3987-21 SPIE Copyright © 2000

- [43] Gierke, T. D.; Munn, G. E.; Wilson, F. C. J. (1981). "The morphology in nafion perfluorinated membrane products, as determined by wide- and small-angle x-ray studies". *Journal of Polymer Science: Polymer Physics Edition* 19 (11): 1687–1704. (1981).
- [44] Connolly D.J.; Longwood; Gresham, W. F. (1966). "Fluorocarbon Vinyl Ether Polymers". U.S. Patent 3,282,875
- [45] Viswanathan B. and Helen M., Is Nafion®, the only Choice?, Viswanathan & Helen, *Bulletin of the Catalysis Society of India*, 6 (2007) 50-66
- [46] J.J. Sumner, S.E. Creager, J.J. Ma and D.D. Desmarteau, *J. Electrochem. Soc.*, 145 (1998)107.
- [47] J. St-Pierre and D.P. Wilkinson, *AIChE J.*, 47 (1998) 1482.
- [48] S. Slade, S.A. Campbell, T.R. Ralph and F.C.Walsh, *J. Electrochem. Soc.*, 149 (2002) A1556.
- [49] Curtin D.E, Lousenberg. R.D, Henry T. J., Tangeman P.C. and Tisack M.E., *Power Sources*, 131(2004) 41.
- [50] Schuster, M., Ise, M., Fuchs, A., Kreuer, K.D., Maier, J. (2005). "Proton and Water Transport in Nano-separated Polymer Membranes". Germany: Max-Planck-Institut für Festkörperforschung, n.d..
- [51] Gelbard, Georges (2005). "Organic Synthesis by Catalysis with Ion-Exchange Resins". *Industrial & Engineering Chemistry Research* 44: 8468–8498. doi:10.1021/ie0580405.
- [52] Gao, L.; Seliskar, C.J. *Chem. Mater.* 1998, 10, 2481.
- [53] Kitsukawa, S. et al. *Chem. Sens.* 1997, 13 (Suppl. A, Proc. 24th Chemical Sensor Symp. 1997), 49.
- [54] Lee, J.H., Lee, J.H., Nam, J.D. Choib, H., Jung, K., Jeon, J.W., Lee, Y.K., Kim, K.J., Tak, Y., "Water uptake and migration effects of electroactive ion-exchange polymer metal composite (IPMC) actuator." *Sensors and Actuators A* (118), 98–106 (2005).
- [55] Gierke, T.D., *J. Electrochem. Soc.* 124 319C, (1977).
- [56] Hsu, W.Y., Timothy, T.D., Gierke, T.D., *Macromolecules* 15, 101, (1982).
- [57] Gierke, T. D., Munn, C. E., and Walmsley, P. N., "The morphology in Nafion perfluorinated membrane products, as determined by wide- and small-angle X-ray studies," *J. Polym. Sci., Polym. Phys. Ed* 19, 1687-1704 (1981).
- [58] Roche, E. J., Pineri, M., Duplessix, R., and Levelut, A. M., "Small-angle scattering studies of Nafion membranes," *J. Polym. Sci., Polym. Phys. Ed* 19(1), 1-11 (1981).

- [59] Xue, T., Trent, J. S., and Osseo-Asare, K., "Characterization of Nafion membranes by transmission electron microscopy," *J. Membr. Sci* 45(3), 261-271, (1989).
- [60] Xue, T., Longwell, R. B., and Osseo-Asare, K., "Mass transfer in Nafion membrane systems: effects of ionic size and charge on selectivity," *J. Membr. Sci.* 58(2), 175-189 (1991).
- [61] James, P. J., Elliott, J. A., McMaster, T. J., Newton, J. M., Elliott, A. M. S., Hanna, S., and Miles, M. J., "Hydration of Nafion (R) studied by AFM and X ray scattering," *J. Mater. Sci.* 35(20), 5111-5119 (2000).
- [62] M. Shahinpoor, Ionic polymer–conductor composites as biomimetic sensors, robotic actuators and artificial muscles—a review, *Electrochim. Acta* 48 (1999) 2343–2353
- [63] M.D. Bennett, D.J. Leo, Ionic liquids as stable solvents for ionic polymer transducers, *Sens. Actuators A Phys.* 115 (2004) 79–90.
- [64] K.J. Kim, M. Shahinpoor, A novel method of manufacturing three dimensional ionic polymer-metal composites (IPMCs) biomimetic, *Sens. Actuators Artif. Muscles Polym.* 43 (2002) 797–802.
- [65] F. Vidal, C. Plesse, Long-life air working conducting semi-IPN/ionic liquid based actuator, *Synth. Met.* 142 (2004) 287–291.
- [66] Leary S and Bar-Cohen Y 1999 Electrical impedance of ionic polymer–metal composites *Proc. SPIE's 6th Annual Int. Symp. Smart Struct. Mater.* 3669 81–6
- [67] Kwang J Kim and Mohsen Shahinpoor, polymer, A novel method of manufacturing three-dimensional ionic polymer-metal composites (IPMC) biomimetics,actuators and artificial muscles,43(2002) 797-802
- [68] Vinh Khanh Nguyena, Jang Woo Lee b, Youngtai Yoo, Characteristics and performance of ionic polymer–metal composite actuators based on Nafion/layered silicate and Nafion/silica nanocomposites, *Sensors and Actuators B* 120 (2007) 529–537
- [69] E.T. Enikov and G.S. Seo, Experimental Analysis of Current and Deformation of Ion-exchange Polymer Metal Composite Actuators, *Society for Experimental Mechanics*,(2005)
- [70] Nemat-Nasser, S., Wu, Y., "Tailoring the actuation of ionic polymer–metal composites," *Smart Mater. Struct.* (15), 909–923 (2006).
- [71] Yoseph Bar-Cohen, Xiaoqi Bao, Shyh-Shiuh Lih, Kaushik Bhattacharya, and Xiao Yu, Characterization of The Electromechanical Properties of IPMC, *Mat. Res. Soc. Symp. Proc. Vol. 698* © 2002 Materials Research Society

- [72] Yoseph Bar-Cohen, Stewart Sherrit and Shyh-Shiuh Lih, Characterization of the Electromechanical Properties of EAP materials, Proceedings of EAPAD, SPIE's 8th Annual International Symposium on Smart Structures and Materials, 5-8 March, 2001, Newport, CA. Paper No. 4329-43
- [73] Takenaka, H., Torikai, E., Kawami, Y., Wakabayashi, N., and Sakai, T., "Solid polymer electrolyte water electrolysis. II. Preparation methods for membraneelectrocatalyst composite," *Denki Kagaku Oyobi Kogyo Butsuri Kagaku*, v.53, no. 4, 1985, p. 261-265.
- [74] Keisuke Oguro, Osaka National Research Institute, AIST, Japan
- [75] Newbury K Characterization, modeling, and control of ionic polymer transducers Dissertation Virginia Polytechnic Institute and State University 2002
- [76] Shahinpoor M 1995 Micro-electro-mechanics of ionic polymer gels as electrically controllable artificial muscles *J. Intell. Mater. Syst. Struct.* 6 307–17
- [77] Nemat-Nasser S and Li J Y 2000 Electromechanical response of ionic polymer–metal composites *J. Appl. Phys.* 87 3321–31
- [78] Tadokoro S, Yamagami S, Takamori T and Oguro K 2000 An actuator model of ICPF for robotic applications on the basis of physicochemical hypotheses *Proc. IEEE Int. Conf. On Robotics and Automation* pp 1340–6
- [79] Kanno R, Tadokoro S, Takamori T and Hattori M 1996 Linear approximate dynamic model of ICPF actuator *Proc. IEEE Int. Conf. on Robotics and Automation* (Piscataway, NJ: IEEE) pp 219–25
- [80] Nemat-Nasser, S., and Li, J. Y. "Electromechanical response of ionic polymermetal composites," *J. Appl. Phys.* V. 87, no. 7, 2000, pp. 3321–3331.
- [81] Nemat-Nasser S 2002 Micromechanics of actuation of ionic polymer–metal composites *J. Appl. Phys.* 92 2899–915
- [82] Nemat-Nasser S 2002 Micromechanics of actuation of ionicpolymer–metal composites *J. Appl. Phys.* 92 2899–915
- [83] Kanno R, Kurata A, Hattori M, Tadokoro S, Takamori T and Oguro K 1994 Characteristics and modeling of ICPF actuators *Proc. Japan–USA Symp. on Flexible Automation* vol 2, pp 691–8
- [84] Xiao Y and Bhattacharya K 2001 Modeling electromechanical properties of ionic polymers *Proc. SPIE* 4329 292–300

- [85] Kanno R, Kurata A, Hattori M, Tadokoro S, Takamori T and Oguro K 1994 Characteristics and modeling of ICPF actuators Proc. Japan–USA Symp. on Flexible Automation vol 2, pp 691–8
- [86] Xiao Y and Bhattacharya K 2001 Modeling electromechanical properties of ionic polymers Proc. SPIE 4329 292–300
- [87] DeGennes P, Okumura K, Shahinpoor M and Kim K 2000 Mechanoelectric effects in ionic gels Europhys. Lett. 40 513–8]
- [88] Gerritsen, M., Kros, A., Sprakel V., Lutterman, J.A., Nolte, R.J.M and Jansen, J.A., Biocompatibility evaluation of sol gel coatings for subcutaneously implantable glucose sensors, Biomaterials, Vol. 21, pp.71–78,2000.
- [89] R.F. Silva, S. Passerini, A. Pozio, Solution-cast Nafion[®]/montmorillonite composite membrane with low methanol permeability, Electrochimica Acta 50 (2005) 2639–2645
- [90] Kim, K. J. and Shahinpoor M., A novel method of manufacturing three-dimensional ionic polymer-metal composites (IPMCs) biomimetic sensors, actuators and artificial muscles, Vol. 43, pp.797–802, 2002.
- [91] Shahinpoor, M. and Kim, K. J., The effect of surface-electrode resistance on the performance of ionic polymer-metal composite (IPMC) artificial muscles, Smart Materials and Structures, 5255-5267,2003. pp.71-78, 2000.
- [92] Nemat-Nasser, S., “Micromechanics of Actuation of Ionic Polymer-metal Composites,” J. Appl. Phys., v. 92, no. 5, 2002, pp. 2899–2915.
- [93] M.D. Bennett, D.J. Leo, Ionic liquids as stable solvents for ionic polymer transducers, Sens. Actuators A: Phys. 115 (2004) 79–90.
- [94] Mohsen Shahinpoor and Kwang J. Kim, Ionic polymer–metal composites: IV. Industrial and medical applications, Smart Mater. Struct. 14 (2005) 197–214
- [95] Shuxiang GUO, Yasuyuki Hasegawa, Toshio Fukuda and Kinji Asaka, Fish-like Underwater Microrobot with Multi DOF, 2001 International Symposium on Micromechatronics and Human Science 2001.
- [96] Tissaphern Mirfakhrai, John D. W. Madden, and Ray H. Baughman, Polymer artificial muscles, Materials Today APRIL 2007, Volume 10, Number 4,2007
- [97] Lee, S., Kim, K.J., Park, H.C, “Modeling of an IPMC Actuator-driven Zero-Net-Mass-Flux Pump for Flow Control,” Journal of Intelligent Material Systems and Structures 17; 533 (2006).
- [98] Keisuke Oguro, Osaka National Research Institute, AIST, Japan, Preparation Procedure Ion Exchange Polymer Metal Composites (IPMC) Membranes

- [99] Oguro, K., Kawami, Y., and Takenaka, H., "An actuator element of polyelectrolyte gel membrane-electrode composite," *Osaka Kogyo Gijutsu Shikensho Kiho*, 43, no. 1, 1992, pp. 21-24.
- [100] Takenaka, H., Torikai, E., Kawami, Y., Wakabayashi, N., and Sakai, T., "Solid polymer electrolyte water electrolysis. II. Preparation methods for membraneelectrocatalyst composite," *Denki Kagaku Oyobi Kogyo Butsuri Kagaku*, v.53, no. 4, 1985, p. 261-265.
- [101] Oguro, K., Fujiwara, N., Asaka, K., Onishi, K., and Sewa, S., "Polymer electrolyte actuator with gold electrodes," *SPIE Proc. Vol. 3669*, 1999, pp. 64-71.
- [102] Kwang J. Kim and Mohsen Shahinpoor, Ionic polymer-metal composites: II.Manufacturing techniques, *Smart Mater. Struct.* 12 (2003) 65–79
- [103] Barbar J. Akle and Donald J. Leo, On the Relationship between the Electric Double Layer and Actuation in Ionomeric Polymer. *Mater. Res. Soc. Symp. Proc. Vol. 855E* © 2005 Materials Research Society.
- [104] C.K. Chung, P.K. Funga, Y.Z. Hong, M.S. Ju , C.C.K. Lin , T.C. Wu , A novel fabrication of ionic polymer-metal composites (IPMC) actuator with silver nano-powders, , *Sensors and Actuators B* 117 (2006) 367–375
- [105] Sang Jun Lee, Man Jae Han, Seong JunKim, JaeYoung Jho, Ho Young Lee and Yong Hyup Kim, A new fabrication method for IPMC actuators and application to artificial fingers, *Smart Mater. Struct.* 15 (2006) 1217–1224
- [106] E.H. Sanders, K.A. McGrady, G.E. Wneka, C.A. Edmondsonb, J.M. Mueller ,J.J. Fontanella , S. Suarez c, S.G. Characterization of electrospayed Nafion films Greenbaumc, *Journal of Power Sources* 129 (2004) 55–61
- [107] Vinh Khanh Nguyena, Youngtai Yoo , A novel design and fabrication of multilayered ionic polymer-metal composite actuators based on Nafion/layered silicate and Nafion/silica nanocomposites *Sensors and Actuators B* 123 (2007) 183–190
- [108] J.D. Nam, H.R. Choi , Y.S. Tak, K.J. Kim, Novel electroactive, silicate nanocomposites prepared to be used as actuators and artificial muscles. *Sensors and Actuators A* 105 (2003) 83–90
- [109] Bennett, M., and Leo, D.J., "Manufacture and characterization of ionic polymer transducers with non-precious metal electrodes," *Smart Materials and Structures*, vol. 12, no. 3, 2003, pp. 424–436.
- [110] B.J. Akle, M.D. Bennett, D.J. Leo, *Proceedings of the 2004 ASME, IMECE conference*, Vol. 61246, 2004

- [111] Kaneda, Y., Kamamichi, N., Yamakita, M., Asaka, K. and Luo, Z. W., Control of Linear Artificial Muscle Actuator Using IPMC, SICE Annual Conference in Fukui, pp.2 18-223, 2003.
- [112] Nemat-Nasser S and Yu Li J 2000 Electromechanical response of ionic polymer–metalcomposites *J. Appl. Phys.* 87 3321–31
- [113] Xue, T., Trent, J. S., and Osseo-Asare, K., “Characterization of Nafion membranes by transmission electron microscopy,” *J. Membr. Sci* 45(3), 261-271, (1989).
- [114] Bandopadhyaya, D., Bhattacharya, B., Dutta, A., “Active Vibration Control Strategy for a Single-Link Flexible Manipulator Using Ionic Polymer Metal Composite,” *J. Intell. Mater. Syst. Struc.* 19, 487–496 (2008).